frontiers | Frontiers in Marine Science

TYPE Original Research
PUBLISHED 22 February 2023
DOI 10.3389/fmars.2023.1118431

OPEN ACCESS

EDITED BY
Paraskevi Polymenakou,
Hellenic Centre for Marine Research (HCMR), Greece

REVIEWED BY
Lech Kotwicki,
Polish Academy of Sciences, Poland
Motohiro Shimanaga,
Kumamoto University, Japan

*CORRESPONDENCE
Thomas Soltwedel
Thomas.Soltwedel@awi.de

†PRESENT ADDRESS
Josephine Z. Rapp,
Department of Biochemistry, Microbiology and Bioinformatics, Université Laval, Quebec, QC, Canada

SPECIALTY SECTION
This article was submitted to Deep-Sea Environments and Ecology, a section of the journal Frontiers in Marine Science

RECEIVED 07 December 2022
ACCEPTED 06 February 2023
PUBLISHED 22 February 2023

CITATION
Soltwedel T, Rapp JZ and Hasemann C (2023) Impact of local iron enrichment on the small benthic biota in the deep Arctic Ocean.
Front. Mar. Sci. 10:1118431.
doi: 10.3389/fmars.2023.1118431

Impact of local iron enrichment on the small benthic biota in the deep Arctic Ocean

Thomas Soltwedel*, Josephine Z. Rapp† and Christiane Hasemann

Deep-Sea Ecology and Technology, Alfred-Wegener-Institute Helmholtz-Center for Polar and Marine Research, Bremerhaven, Germany

This study assesses the impact of local iron enrichment on the small benthic biota (bacteria, meiofauna) at the deep seafloor. To evaluate the hypothesis that abundance, distribution, and diversity of the small benthic biota varies in relation to a local input of structural steel at the seabed, we analyzed sediment samples and the associated infauna along a short transect (~1.5 m in length) with increasing distance to an iron source, i.e., corroding steel weights (30 cm in length and width, and 6 cm in height) of a free-falling observational platform (bottom-lander), lying on the seafloor for approximately seven years. Bacterial and meiofaunal densities and biomasses in iron-enriched sediments were significantly lower than those in unaffected sediments. Moreover, bacterial and nematode community structure between iron-enriched sediments and unaffected sediments differed strongly; taxonomic richness as well as diversity was lowest closest to the iron source. The presence of iron fostered the establishment of specialized iron oxidizers and other chemolithoautotrophic bacterial members, which were rare or absent in the unaffected sediments, within which opportunistic heterotrophs predominated. Nematodes comprised >90% of the total metazoan meiofauna and were therefore studied in more detail. A total of 26 genera from 16 families occurred in iron-enriched sediments (three genera were found exclusively in these sediments), while 65 genera from 27 families occurred in the unaffected sediments (39 genera and 12 families were found exclusively in these sediments). Nematode genera number (S), estimated genera richness ($EG_{(51)}$) and heterogeneity ($H'_{(log2)}$) were significantly lower in iron-enriched sediments than in unaffected sediments. Our results confirm that the local enrichment of deep-sea sediments by metallic and corroding structures (e.g., by ship hulls, containers, scientific equipment) strongly affects the diversity of the small benthic biota at short distances from these sources.

KEYWORDS

deep sea, sediments, iron, bacteria, meiofauna, nematoda, LTER HAUSGARTEN

Introduction

According to the latest Allianz Global Corporate and Specialty (AGCS) Safety and Shipping Review (Allianz Global Corporate & Specialty, 2022), the number of total shipping losses (sunken ships and constructive total losses) is continuously declining; driven by improved regulation and the development of a more robust safety culture, large shipping losses have dropped by more than 57% over the past decade. Still, in 2021, the maritime industry registered 54 large ship losses (vessels of ≥100 gross tons), locally introducing huge quantities of iron and steel to the seabed. Cargo vessels account for 27% of 2021's losses, with containers transported by these vessels and lost at sea in bad weather conditions representing another source for the local input of large quantities of structural steel. Recently, the World Shipping Council (WSC) estimated that there were on average 1,629 containers lost at sea each year for the period 2008-2021 (WSC, World Shipping Council, 2022), while environmental associations estimate a much higher number of up to 20,000 lost containers per year. Regardless of their load and exterior coatings, which may be toxic to organisms, all these large steel structures will take centuries to degrade at the deep seafloor (Kuroda et al., 2008; Melchers, 2019).

Like natural structures (sessile organisms, sunken wood, dropstones), sunken ships and/or their load introduce habitat heterogeneity at the soft-bottom seafloor, creating artificial reefs and potentially increasing biodiversity (Buhl-Mortensen et al., 2010; Meyer et al., 2016). Taylor et al. (2014), studying deep-sea faunal communities associated with a lost shipping container at 1,281 m water depth in Monterey Bay off NW America, could show that after seven years at the seafloor, macro- and megafaunal assemblages on the container and in the immediate vicinity (≤ 10 m) differed significantly from those found at distances of up to 500 m from the box. However, to our knowledge, the impact of human iron and steel debris on the small benthic biota, in the size range from bacteria to meiofauna has so far never been investigated.

Compared to huge metal structures like sunken ships or lost containers, bottom-weights of freefalling scientific platforms, so-called bottom-landers (Tengberg et al., 1995), left at the seafloor after recovery of a research platform, represent a comparably minor impact on seafloor communities, but are well suited to study the reaction of benthic bacteria and meiofauna to corroding steel structures that have reached the seabed.

Corrosion is caused by complex chemical, physical and biological processes (Kip and Veen, 2015). Primary factors that affect the rates and mechanisms of corrosion in seawater rarely vary and include the surrounding seawater's salinity, dissolved oxygen concentration, pH, temperature, and bottom currents, which in turn affect the prevalence of other parameters (Moore III, 2015). However, especially in anoxic marine environments, activities of sulfate-reducing bacteria inhabiting the upper sediment layers can significantly promote the formation of corrosion products, if an appropriate organic food source is present (Castaneda and Benetton, 2008). Consequently, corroding iron at the seafloor should most probably affect the composition of bacteria in adjacent sediments, with cascading effects on meiofauna assemblages feeding on sediment-inhabiting bacteria.

To study the impact of iron enrichment on the small benthic biota (bacteria, meiofauna) at the deep seafloor, we retrieved sediment samples along a short transect (~1.5 m in length) with increasing distance to an iron source, i.e., the corroding steel weights (30 cm in length and width, and 6 cm in height) of a free-falling observational platform (bottom-lander) lying at the seafloor for about seven years. With our study we evaluate the hypothesis that the abundance, distribution, and diversity of the small benthic biota varies in relation to a local input of structural steel at the seabed.

Material and methods

Iron-enriched surface sediments formed in the vicinity of a bottom-weight left in summer 2008 after a short-term deployment of a bottom-lander in 2,433 m water depth at the LTER (Long-Term Ecological Research) observation HAUSGARTEN (Soltwedel et al., 2016) on the eastern flank of the Fram Strait were sampled on 28th July 2015 from on board of RV *Polarstern* (Alfred-Wegener-Institut Helmholtz-Zentrum für Polar- und Meeresforschung, 2017). The block-shaped steel bottom-weights (30 x 30 x 6 cm; Figure 1) were sitting with roughly half of the 6 cm height sunken into the seafloor and thus, the weights would have a negligible effect on near-bottom currents. During sampling in 2015, the bottom-weights were largely corroded in the high saline (~34.8 ‰) and oxygen saturated (~310 µmol L^{-1}) bottom waters. Surface sediments around the weights had an orange-red color that gradually decreased in color intensity with increasing distance from the source, i.e., the bottom-weights (Figure 1). Sediment sampling was carried out using push-corers (PC) handled by the Remotely Operated Vehicle (ROV) *QUEST 4000* (MARUM Center for Marine Environmental Sciences, Germany). A total of eight push-corer samples (PC1-8) were taken at approx. regular distances (on average every 18 cm) along a short transect (about 1.5 m) crossing the iron gradient. Push-corers PC1-4 retrieved sediment from heavily iron impacted sediments, whereas samples taken from push-corers PC5-8 were visually indistinguishable from background sediments in the wider area. After recovery of the ROV, sediment cores (8 cm in diameter, and 20-25 cm in height) were sub-sampled for various parameters (see below) using plastic syringes with cut-off anterior ends.

Sample processing for sediment-inhabiting bacteria

Two 5-ml syringes (1 cm in diameter) from each core were taken for determining bacterial numbers and biomasses. Subsamples were sectioned in 1-cm layers down to 5 cm sediment depth and analyzed individually. Bacterial cells were counted by epifluorescence microscopy after staining with acridine orange according to Meyer-Reil (1983). Volumetric determinations were conducted with the Porton grid as described by Grossmann and Reichardt (1991). Bacterial biomass was estimated using a conversion factor of 3.0 x 10^{-13} g C $µm^{-3}$ (Børsheim et al., 1990).

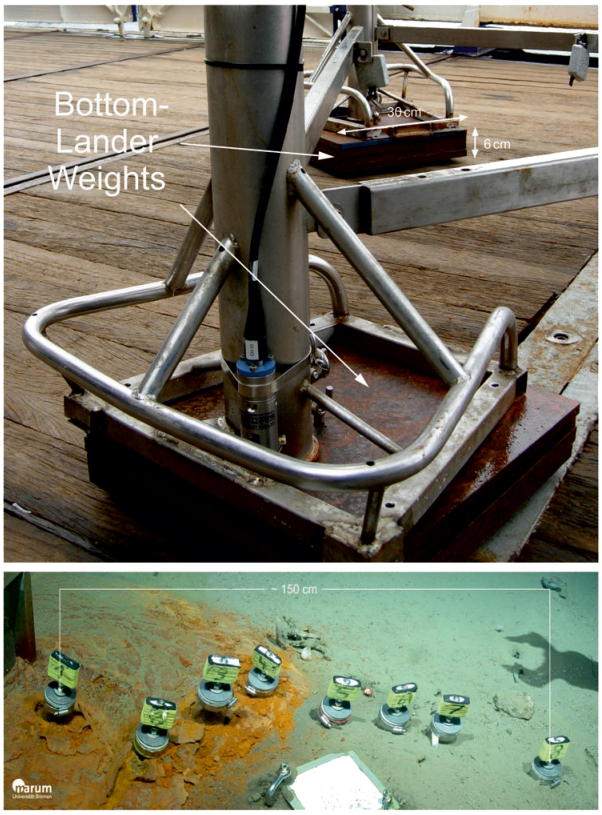

FIGURE 1
Block-shaped steel weights of a bottom-lander (above) and sediment sampling along a gradient with decreasing iron concentrations in the vicinity of corroding bottom-weights (below) using push-corers (PC1-8) handled by a Remotely Operated Vehicle *QUEST 4000* (© MARUM).

One 20-ml syringe from each push-core was taken for DNA sequencing. Prior to DNA extraction, sediment subsamples were sliced into 1-cm sections down to 5 cm sediment depth. For each depth, total community DNA was extracted from 1 g of wet sediment using the PowerSoil DNA Isolation Kit (MoBio Laboratories, Solana Beach, CA, USA) according to the manufacturer's instructions. For PC1-4, where a thick crust of iron oxides covered the sediment, 1 g of wet iron crust fragments was used for extraction. DNA extracts were stored at -20°C until sequencing.

Amplicon sequencing was performed on an Illumina MiSeq machine at the CeBiTec laboratory (Center for Biotechnology, Bielefeld University). The bacterial primers 341F (5′-CCTACGGGNGGCWGCAG-3′) and 785R (5′-GACTAC HVGGGTATCTAATCC-3′) were used generate of 16S rRNA gene libraries targeting the v3–v4 hypervariable region (fragment length 400-425 bp) (Klindworth et al., 2013). Libraries were sequenced with MiSeq v3 chemistry in 2 bp×300 bp paired runs according to the 16S Metagenomic Sequencing Library Preparation protocol (Illumina, Inc., San Diego, CA, USA). A total of ~86,000 - 203,000 raw reads per sample were obtained (Supplement Table S1) and archived in the European Nucleotide Archive (ENA) under project accession number PRJEB57769.

For sequence processing, a modularized workflow was applied that combines multiple software tools and custom scripts[1]. In a first step, primers were clipped using *cutadapt* v1.9.1 (Martin, 2011), allowing an error rate of up to 16% and no indels. Subsequently low-quality sequences were removed using *trimmomatic* v0.32 (Bolger et al., 2014) with SLIDINGWINDOW:4:15 MINLEN:100. The remaining paired reads with a minimum overlap of 20 bp were merged using *PEAR* v0.9.6 (Zhang et al., 2014). Only merged sequences of 350-500 bp in length were used for further analysis. The remaining sequences passed the quality control in *FastQC* v0.11.4 (Andrews, 2010), with a mean sequence quality (phred score) of >36.

For the clustering of sequences into operational taxonomic units (OTUs) we used the *swarm* algorithm v2.1.1 (Mahé et al., 2015) in the fastidious mode with default settings. Representative sequences of each OTU were submitted for taxonomic classification to the NGS analysis pipeline of the SILVA rRNA gene database project (SILVAngs 1.3) (Quast et al., 2013), skipping the internal clustering and using the SSU Ref NR99 132 for classification.

Absolute singletons, i.e., OTUs represented by only a single sequence across the full dataset (Gobet et al., 2014) as well as all OTUs classified outside the bacterial domain, i.e., chloroplast, mitochondrial or archaeal sequences, were removed from the dataset. An overview of the number of sequences retained after each processing step is given in Supplementary Table S1.

Sample processing for sediment-inhabiting meiofauna

One 20-ml syringe (2 cm in diameter) from each core was taken for meiofauna analyses, including foraminiferans and metazoans. As for bacterial investigations, sediment cores were sectioned in 1-cm layers down to 5 cm sediment depth. After staining in Rose Bengal for 24 h, single sediment layers were passed through a set of sieves with various mesh sizes (1000, 500, 250, 125, 63, and 32 µm) to facilitate further processing (see Pfannkuche and Thiel, 1988). All organisms that passed through the 1.0 mm sieve, were enumerated under a low-power stereo microscope. Organisms were identified to major taxonomic groups. For statistical analyses (see below), all taxa appearing in minor quantities (e.g., harpacticoids, polychaetes, ostracods, kinorhynchs, bivalves, gastropods, tanaidaceans, and tardigrades) were pooled into one category, classified as "Others". Meiofaunal densities were standardized to individuals per 10 cm^2.

Nematodes comprised >90% of the total metazoan meiofauna and were therefore studied in more detail. All nematodes found in the samples were transferred to anhydrous glycerol and mounted on permanent slides for further studies (De Grisse, 1969). Nematodes were identified to genus level (Schmidt-Rhaesa, 2014). The classification into different feeding types was done according to 1960; Wieser (1953). Groups IA and IB describe selective and non-selective deposit feeders without teeth. Groups IIA and IIB comprise epigrowth feeders as well as predators and omnivores

1 https://github.com/chassenr/NGS/blob/master/AMPLICON/illumina16Sworkflow_master.txt.

with teeth. The groups of deposit feeders (IA and IB) mainly consume bacteria and small-sized (IA) or larger-sized organic particles (IB). Epigrowth feeders (IIA) use their teeth to tap objects or scrap off surfaces for food. Predators and omnivores (IIB) also tap plant objects, but the most important feeding mode is predation or scavenging by using their buccal armature to feed on nematodes or other small invertebrates (Soeteart and Heip, 1995).

In addition, each nematode specimen was assigned to certain life-history characteristics. The Maturity index MI (Bongers, 1990; Bongers et al., 1991) is represented by a colonizer-persister (c-p) value that ranges from a colonizer (c-p = 1) to a persister (c-p = 5) with the index values representing life-history characteristics associated with r- and K-selection, respectively (Bongers et al., 1995; Bongers and Bongers, 1998; Bongers and Ferris, 1999).

Nematode biomasses were estimated from digital microscope images of individual nematodes using the *cellP* software (Olympus®). The length (excluding filiform tails) and width (at the widest part of the body) of each nematode specimen was measured using the software's *Polygon* measurement tool. With this tool, any number of (anchoring) points can be set to trace curves and body twists of the nematode specimen with the mouse pointer. Nematode wet weight (WW) was calculated following Andrassy (1956): $WW(\mu g) = (LxW^2)/Cf$, with L [µm] = nematode's length, W [µm] nematode's width at the widest point and Cf = conversion factor that equals 1.6×10^6.

The taxonomic identification and measurements (length and width) of the nematode specimens was done using light microscopy (up to 100-times magnification, with Nomarski optic). Nematode diversity was quantified using the rarefaction method (Hurlbert, 1971) for a sample of 51 individuals ($EG_{(51)}$), Pielou (1969) evenness measure J' and by combining aspects of species richness and evenness as heterogeneity, based on the Shannon-Wiener index $H_{(log2)}$ (Shannon and Weaver, 1963).

Sample processing for sediment parameters

One 5-ml syringe (1-cm in diameter) from each core was analyzed for iron concentrations; the subsample from push-corer PC1 was lost during analyses. The bulk metal composition of the sediments was determined after total acid digestion as described in Nöthen and Kasten (2011) and Volz et al. (2020). Approximately 75 mg of freeze dried and powdered sediment was dissolved in a mixture of 65% distilled HNO_3 (3 ml), 32% distilled HCl (2 ml) and 40% HF of suprapur® grade (0.5 ml) by use of a CEM Mars Xpress microwave system. The acids were subsequently fumed off and the residue was re-dissolved in 5 ml 1M HNO_3. The solution was then topped up with 1M HNO_3 to a volume of 50 ml and analyzed on an iCAP 7400 ICP-OES instrument. Yttrium was applied as an internal standard to correct for physical differences of samples.

Sediment samples taken from each push-corer with 20-ml syringes were split vertically into equal parts. One half was analyzed for the water content as a proxy for the porosity of the sediments and to determine the organic matter content. The second half was used to determine chloroplastic pigments, indicating food/energy availability from phytodetritus sedimentation. Water contents (H2O) were determined by measuring the weight loss of wet sediment samples dried for 48 h at 60°C. The total organic matter content of the sediments was estimated as ash-free dry-weight (AFDW) after combustion of sediment samples for 2 h at 500°C. Chloroplastic pigments (chlorophyll *a* [CHL] and its degradation products, i.e., phaeopigments) were extracted in 90% acetone and measured with a TURNER fluorometer (Shuman and Lorenzen, 1975). The bulk of pigments, defined as chloroplastic pigment equivalents, CPE (Thiel, 1978).

Statistical community analyses

For the bacterial community analyses, we performed all statistical analysis and visualization of results in R v3.6.1 (R Core Team, 2017). For alpha-diversity analysis, we used the *estimateR* and *diversity* functions implemented in the *vegan* package v.2.5.6 (Oksanen et al., 2019) on random, rarefied subsamples (n=100) to the smallest sample size (13,280 sequences). We used *ampvis2* v.2.5.8 (Andersen et al., 2018) to visualize community composition and for the creation of the two-dimensional non-metric multidimensional scaling (NMDS) ordination of sample dissimilarities. The underlying dissimilarity matrix was calculated using the Bray-Curtis distance measure on the basis of OTU relative abundances. To test whether between-group differences in community structure were larger than within-group differences, we performed an Analysis of Similarity (ANOSIM) with 999 permutations. We performed Welch t-tests using the *stats4bioinfo* R package to identify differences in alpha-diversity and community composition between sample means of iron-impacted (PC1-4) and visually unaffected sediments (PC5-8), and used multiple testing correction to identify significant differences, which passed the false discovery rate (FDR) correction with a corrected P value <0.05 (Benjamini and Hochberg, 1995). We used the *ggplot2* package v3.3.2 (Wickham, 2016) for plotting of results.

For the nematode community analyses, non-metric multidimensional scaling (NMDS) plots were used to visualize multivariate patterns. Similarity matrices for the nematode community structure analysis based on square root-transformed abundance data were built using Bray-Curtis similarity (Clarke and Gorley, 2015). Significance tests for differences in nematode community structure between ferrous and non-ferrous sediments were performed using the one-way ANOSIM test. The SIMPER routine was used to identify which nematode genera were responsible for observed differences in nematode community structure.

Relationships between environmental/food-related variables and nematode community structure were analyzed using distance-based linear models (DistLM) with specified regression as selection procedure, using adjusted R^2 as selection criterion (McArdle and Anderson, 2001; Anderson et al., 2008). The resemblance matrices (Bray-Curtis similarity) of bacterial and nematode community data were based on square-root transformed abundance data of the taxa. The predicting environmental variables incorporated into the distanced-based model were iron concentrations (Fe), bacterial numbers (BN), chlorophyll *a* concentrations (CHL), ash-free dry-weights (AFDW) and water contents (H2O); for the analysis of the

bacterial community, the variable BN was excluded from the model. Normality and collinearity of the predictor variables were assessed using a draftsman plot (Anderson et al., 2008). No pair of variables was correlated by R > 0.6 and hence all variables were retained for possible inclusion in the model. Results of the DistLM were visualized by distance-based redundancy plots (dbRDA), overlaid with normalized predictor variables (Anderson et al., 2008). We used the seriation test of the RELATE routine for comparing resemblance matrices of environmental/food related data with bacterial and nematode community data. A permutation test (9,999 permutations) was used to evaluate significance. If $|0.8 \leq \rho \leq 1.0|$ (where, ρ is the Spearman's correlation), there is a clear trend in the trajectories of the community composition. Welch t-tests were applied in order to test differences in univariable measures of meiofauna communities and environmental/food related variables from ferrous and non-ferrous sediments.

Nematode community taxonomic structure, c-p classes and MI, ITD, and H' values were selected as environmental quality indicators in the present study. Environmental quality was ranked (High > Good > Moderate > Poor > Bad) according to the thresholds proposed by Moreno et al. (2011); Semprucci et al. (2014a; 2014b) and Hua et al. (2021). The thresholds are listed in Table 1.

All multivariate analyses of the nematode community attributes were conducted using statistical routines in the multivariate software package PRIMER-e version 7.0.13 with PERMANOVA (Anderson et al., 2008; Clarke et al., 2014; Clarke and Gorley, 2015) and R v3.6.1 (R Core Team, 2017). Univariate statistical analyses were performed with the TIBCO Statistica 13.3 software (TIBCO, 1984–2017).

Results

Iron concentrations, porosity, organic matter contents, and pigment concentrations

Concentrations of iron in the uppermost 5 cm of the sediments in PC2-4 (mean value for 0-5 cm: 625 ± 142 mg Fe g^{-1}; sediments from PC1 lost during analyses) were significantly higher (t-test: t (33) = 3.9602, p = 0.0004) than those in PC5-8 (mean value for 0-5 cm: 187 ± 6 mg Fe g^{-1}) and sharply decreased from 528 ± 79 mg Fe g^{-1} to 178 ± 5 mg Fe g^{-1} between PC4 and PC5 (Figure 2). As expected, Fe concentrations in unaffected deep-sea sediments showed almost no differences with increasing sediment depth, while sediments influenced by the corroding bottom-weights exhibited pronounced gradients, with iron concentrations close to the ambient at the deepest sediment layer investigated in this study (4-5 cm); the steepest gradient with approx. 8-times higher values in the uppermost centimeter was found in PC3 (Figure 3; Supplement Table S2).

Water contents (H2O) along the push-corer transect (Figure 2) were almost constant with slightly (non-significantly) higher values in iron-enriched sediments at PC1-4 (mean value for 0-5 cm: 54.2 ± 2.9%), compared to unaffected sediments at PC5-8 (mean value for 0-5 cm: 51.4 ± 0.7%). Total organic matter contents (AFDW; Figure 2) were non-significantly higher (p = 0.434) at PC1 (mean value for the uppermost 5 cm of the sediments: 198.1 µg cm^{-3}), compared to AFDW in sediments of PC2-8 (range: 76.6 - 102.8 µg cm^{-3}; mean: 92.5 ± 10.8 µg cm^{-3}). Gradients of H2O and AFDW in the uppermost 5 cm of the sediments were generally rather variable (Figure 3) with overall decreasing values with increasing depth for water contents and slightly increasing values for organic matter contents, except for PC1 where higher AFDW were found at the surface compared to deeper sediment layers (Figure 3). Lowest total pigment concentrations (5.8 µg CPE cm^{-3}) were found at PC1, while highest CPE concentrations were registered at PC4 (12.8 µg CPE cm^{-3}) and PC5 (11.0 µg CPE cm^{-3}); all other sediment cores exhibited intermediate values of approx. 9.5 µg CPE cm^{-3} (Figure 2; Supplement Table S2). While at PC5-8, pigment concentrations in the uppermost five centimeters of the sediments showed gradually declining values with increasing depth, PC1-4 exhibited subsurface maxima at 3-4 cm sediment depth (Figure 3).

Bacterial densities and biomasses

Bacterial numbers in iron-enriched sediments PC1-4 (mean value for 0-5 cm: 0.89 x 10^8 ± 0.11 x 10^8 cells cm^{-3}) were significantly lower (t-test: t(38) = -6.6833, p =0.0001), compared to those in visually unaffected sediments (PC5-8; mean value for 0-5 cm: 1.96 x 10^8 ± 0.24 x 10^8 cells cm^{-3}), but generally decreased with increasing sediment depth (Figure 4; Supplement Table S2). Bacterial biomass followed the same trend with 2-times higher values in unaffected sediments (PC5-8; mean value for 0-5 cm: 52.96 ± 7.82 µg C cm^{-3}), compared to iron-enriched sediments (PC1-4; mean value for 0-5 cm: 25.40 ± 5.35 µg C cm^{-3}; Figure 4; Supplement Table S2). Intriguingly, bacterial densities and biomasses in PC5 showed the

TABLE 1 Thresholds of nematode community descriptors as environmental quality indicators.

Indicator	Bad	Poor	Moderate	Good	High	Source
MI	≤2.2	2.2<MI<2.4	2.4<MI<2.6	2.6<MI<2.8	>2.8	Moreno et al., 2011
c-p 2 and 4	cp2>80%	cp2>60% and cp4<3%	cp2≥50% and cp4 3-10%	cp2≥50% and cp4>10%	cp2≤50% and cp4>10%	Moreno et al., 2011
c-p 1 + 2	80-100%	60-80%	40-60%	20-40%	0-20%	Semprucci et al., 2014a, Semprucci et al., 2014b
c-p 3-5	0-20%	40-20%	60-40%	60-80%	80-100%	Semprucci et al., 2014a, Semprucci et al., 2014b
H'	0<H'≤1	1<H'≤2.5	2.5<H'≤3.5	3.5<H'≤4.5	H'>4.5	Moreno et al., 2011
ITD	1	0.6<ITD≤0.8	0.4<ITD≤0.6	0.25<ITD≤0.4	0.25	Moreno et al., 2011

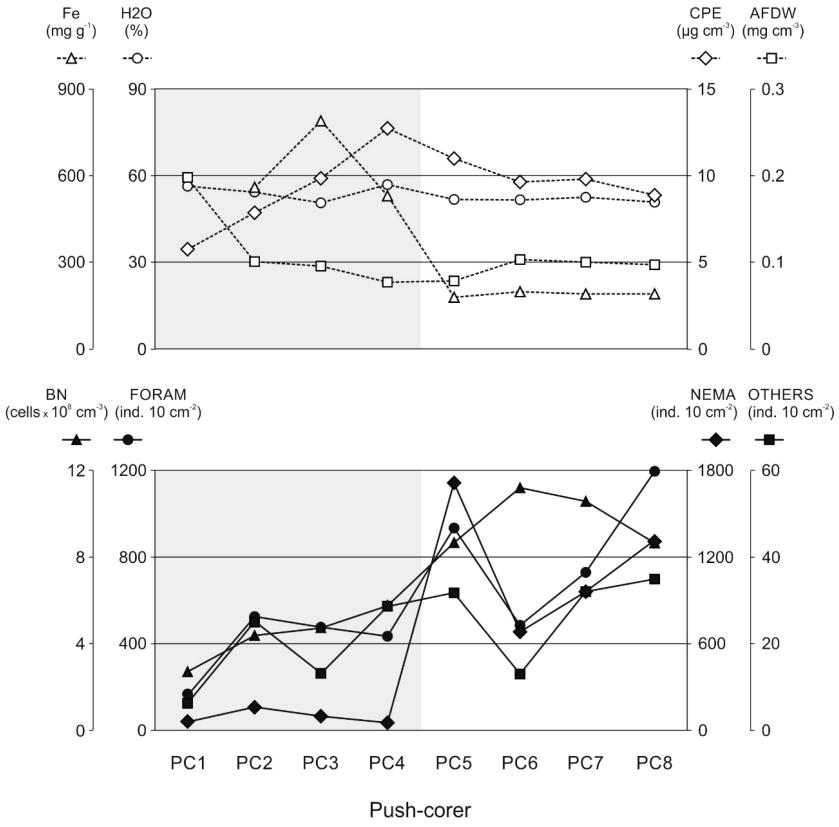

FIGURE 2
Sediment characteristics (upper panel) and densities of the small benthic biota (lower panel) along the push-corer transect. Fe: iron concentrations (no data for PC1), H2O: water contents (porosity), AFDW: organic matter contents, CPE: chloroplastic pigment equivalent concentrations, BN: bacterial densities, FORAM: Foraminifera, NEMA: Nematoda, and OTHERS: all other metazoan meiofauna. Grey shading: visually iron-impacted sediments.

highest values compared to all other samples in the uppermost 2 cm of the sediments, while at deeper sediment depths cell numbers were comparable to those found for PC4.

Bacterial communities

Bacterial community structure between iron-enriched sediments (PC1-4) and visually unaffected sediments (PC5-8) (ANOSIM: R = 0.63, p = 0.001) differed strongly; taxonomic richness, both observed (nOTU) and estimated (chao1), as well as diversity (inverse Simpson and Shannon diversity indices) were significantly lower in iron-enriched sediments than in unaffected sediments, and particularly low in the uppermost centimeter of PC1-3 (Supplement Figure S1 and Table S3). However, communities in PC1-4 were more heterogeneous in structure across the five sampled depth horizons, resulting in a wide scatter of individual samples when visualized in a non-metric multidimensional scaling (NMDS) plot (Figure 5A). Differences in structure appeared most pronounced between the upper layers of the iron-enriched sediments and the more homogenous cluster of unaffected sediments (PC5-8), while communities in the deeper layers of PC1-4 plotted closer to PC5-8.

The classes Gammaproteobacteria, Alphaproteobacteria, Bacteroidia, Deltaproteobacteria, and Acidimicrobiia dominated bacterial communities in both iron-enriched and visually unaffected sediments, yet with significant variability in the relative distribution of Bacteroidia and Acidimicrobiia. The strongest significant discrepancy in relative abundance, however, was apparent for the classes Zetaproteobacteria (5% in PC1-4, 0% in PC5-8) and Campylobacteria (2% in PC1-4, 0% in PC5-8), which were dominant in the iron-enriched sediments, but mostly absent from the rest.

More refined insights into taxa distribution at the resolution of individual genera revealed a clear division of dominant members between iron-impacted and visually unaffected sediments (Table 2; Supplement Figure S2). Genera that were dominant in PC1-4, i.e., genera of >0.5% mean relative abundance, and differentially abundant included *Colwellia*, *Cycloclasticus*, *Gallionella*, and *Oleiphilus* from the Gammaproteobacteria, *Geopsychrobacter* from the Deltaproteo bacteria, *Lutibacter* from the Bacteroidia, Roseobacter clade NAC11-7 lineage from the Alphaproteobacteria, as well as *Mariprofundus* from the Zetaproteobacteria and *Sulfurospirillum* from the Campylobacteria (Supplement Figure S2).

Several dominant members were identified in visually unaffected sediments, whose relative abundance was significantly reduced under the influence of iron, including AqS1, *Nitrosomonas* and *Woeseia* from the Gammaproteobacteria, *Nitrospina* from the Nitrospinia, *Nitrospira* from the same-named class, *Pelagibius* from the Alphaproteobacteria, Subgroup 10 from the

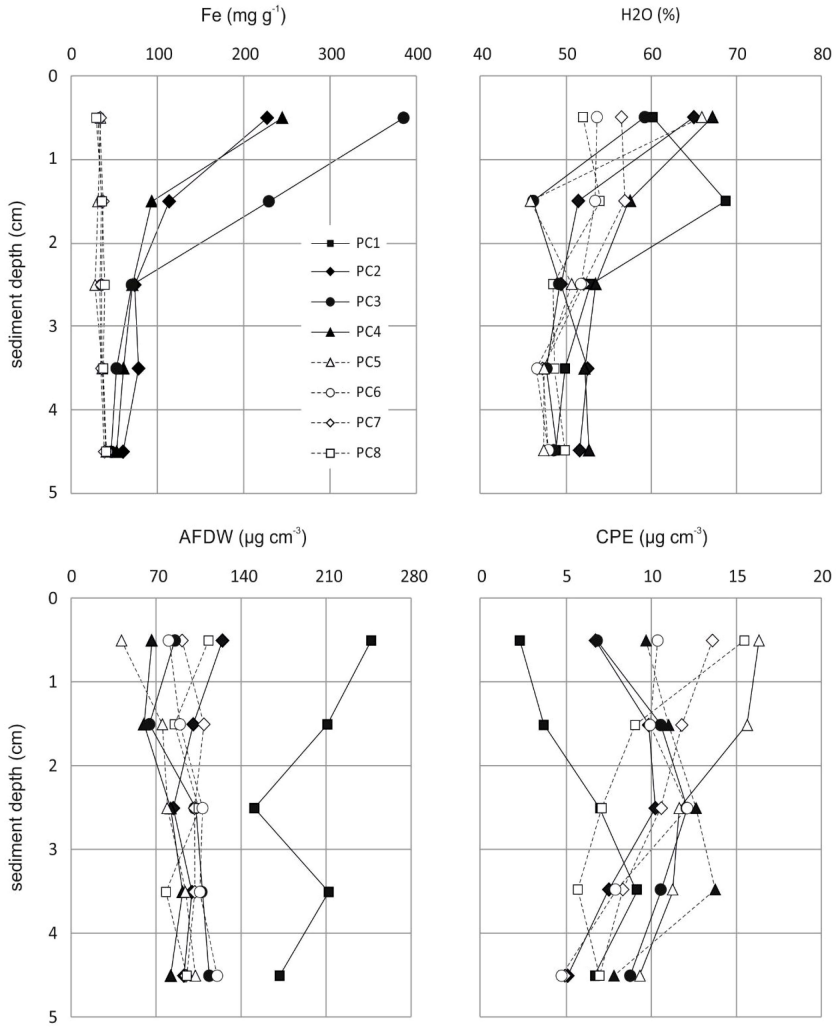

FIGURE 3
Gradients in iron concentrations (Fe; top left), water contents (H2O; top right) and organic matter contents (AFDW: bottom left; CPE: bottom right) in surface sediments along the transect with increasing distance from the corroding bottom-weights (no data for iron concentrations at PC1).

Thermoanaerobaculia, Sva0996 marine group from the Acidimicrobiia and Urania-1B-19 marine sediment group from the Phycisphaerae (Supplement Figure S2). With the exception of *Woeseia*, few genera in the visually unaffected sediments exceeded 3% relative abundance, and overall community composition was more even compared to PC1-4. Here, several instances were observed, where individual genera contributed >20% to total community composition, i.e., *Mariprofundus*, *Gallionella* and *Lutibacter* (Table 2), in line with the lower observed diversity in iron-enriched sediments (Supplement Figure S1).

Heatmap of the dominant community members along the sampled transect. Displayed are average values (%) per push-core, integrating the surface sediment from 0-5 cm depth. Only genera with a minimum relative abundance of 0.1% are shown (all values below 0.1% but above 0.01% still show pale colours). Asterisks indicate significant variance between means of iron-impacted (PC1-4) and unaffected (PC5-8) sediment communities (FDR adjusted p-values: *p>0.05, **p>0.01, ***p>0.001).

Meiofauna major taxa

Total meiofauna densities (including Foraminifera) in iron-enriched sediments (PC1-4) were significantly (t-test: t(38) = 2.7631, p = 0.0088) lower (mean value for 0-5 cm: 514 ± 205 ind. 10 cm^{-2}), compared to those in visually unaffected sediments (PC5-8; mean value for 0-5 cm: 2,021 ± 717 ind. 10 cm^{-2}; Figure 2). This result was primarily due to huge differences in the abundance of foraminiferans and especially nematodes, while all other meiofauna taxa (grouped in the category "Others") showed only slightly (non-significantly) lower values in iron-enriched sediments (6 ± 3 ind. 10 cm^{-2} in PC1-4 compared to 9 ± 3 ind. 10 cm^{-2} in PC5-8).

Meiofauna numbers generally decreased with increasing sediment depth, however, surface layers (0-1 cm) in unaffected sediments (PC5-8) exhibited on average 14-times higher meiofauna densities compared to the deepest sediment layer investigated (4-5 cm), while meiofauna densities in iron-enriched sediments (PC1-4) showed only 3-times higher values.

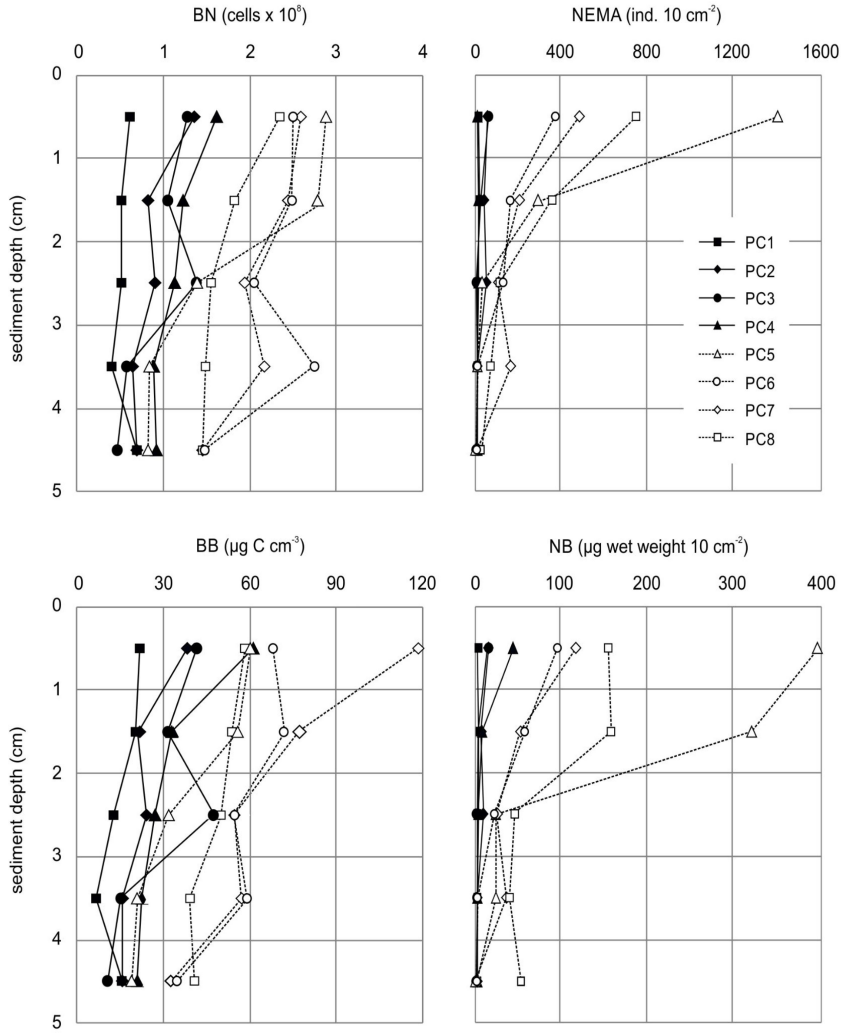

FIGURE 4
Gradients of bacterial numbers (BN; top left) and nematode densities (NEMA; top right) as well as bacterial biomass (BB; bottom left) and nematode biomass (NB; bottom right) in surface sediments along the transect with increasing distance from the corroding bottom-weights.

Meiofauna taxa grouped in the category "Others" showed the steepest gradient in all push-cores (independent of the iron-concentration in the sediments), while foraminiferans exhibited a conspicuous subsurface maximum at 1-2 cm sediment depth in iron-enriched sediments and a regular decrease in relative abundance in unaffected sediments.

The relative abundance of Foraminifera, Nematoda, and the bulk of all other metazoan meiofauna (OTHERS) in the different sediment layers (1. - 5. cm) showed higher proportions of foraminiferans (52 - 87%) compared to the nematodes (7 - 40%) in the uppermost two centimeters in PC1-4, and reverse conditions with greater proportions of nematodes (48 - 75%) compared to foraminiferans (24 - 51%) in PC5-8. At deeper sediment layers (3. - 5. cm), the relative abundance of foraminiferans increased from PC1 to intermediate PCs along the transect and decreased again towards PC8; nematodes showed an inverse trend. The proportion of OTHERS was highest in the uppermost centimeter of PC1-4, ranging between 8% and 16% of the total meiofauna.

Nematode densities and biomasses

The number of nematodes largely followed the trend also observed for bacterial numbers, with significant (t-test: $t(38) = 2.8440$, $p = 0.0071$) lower numbers of nematodes in the iron-enriched sediments (PC1-4; mean value for 0-5 cm: 93.11 ± 50.42 ind. 10 cm^{-2}) than in the non-iron-affected sediments (PC5-8; mean value for 0-5 cm: 1,136.36 ± 451.21 ind. 10 cm^{-2}; Figure 2). Nematode numbers generally decreased with increasing sediment depth; this trend was more pronounced in the unaffected sediments compared to within the iron-enriched sediments (Figure 4; Supplement Table S2). Nematode biomass showed the same pattern as nematode numbers, with biomass values peaking at seven times higher in sediments unaffected by iron (PC5-8; mean value for 0-5 cm: 47.37 ± 37.30 µg C 10 cm^{-2}) compared to iron-enriched sediments (PC1-4; mean value for 0-5 cm: 6.47 ± 9.37 µg C 10 cm^{-2}) (Figure 2; Supplement Table S2). PC5 exhibited the highest values in the uppermost centimeter of the sediment and the steepest

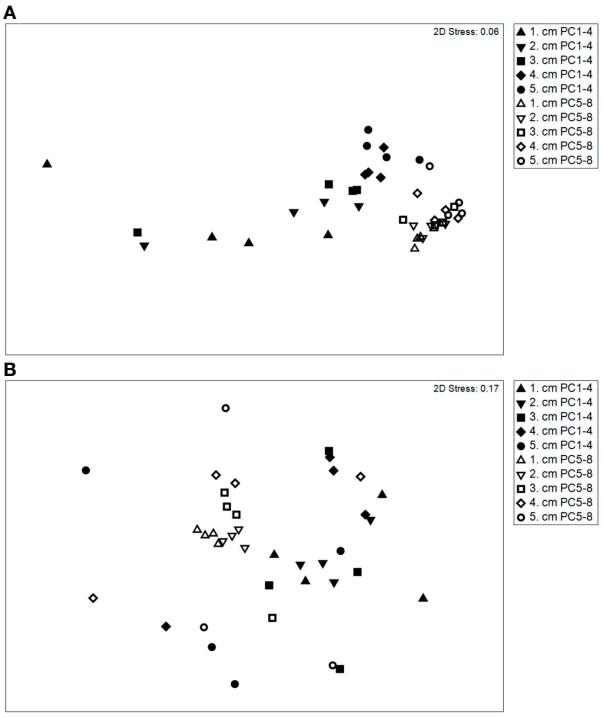

FIGURE 5
Non-metric multidimensional scaling (NMDS) based on similarity matrix (square-root transformed data, Bray-Curtis similarity) of bacteria **(A)** and nematode genera **(B)** abundance in iron-enriched (PC1-4) and unaffected (PC5-8) sediments.

gradient in nematode density and biomass decrease with increasing sediment depth (Figure 4). In deeper sediment layers, the values for nematode density and biomass from the visually unaffected sediments increasingly decreased to the level of the values for iron-enriched sediments; in the deepest sediment layer investigated (4-5 cm), the values showed almost no differences between influenced and uninfluenced sediments (Figure 4).

Nematode communities

Nematode community structure between iron-enriched sediments (PC1-4) and visually unaffected sediments (PC5-8) (ANOSIM: R = 0.26, p = 0.0001) differed strongly. A total of 26 genera from 16 families occurred in iron-enriched sediments (PC1-4, 0-5 cm), three genera were found exclusively in sediments from PC1-4. 65 genera from 27 families occurred in the unaffected sediments (PC5-8, 0-5 cm), 39 genera and 12 families were found exclusively in the sediments of PC5-8.

Genera number (S), estimated genera richness ($EG_{(51)}$) and heterogeneity ($H'_{(log2)}$) were significantly lower in iron-enriched sediments than in unaffected sediments (t-tests: S: t(38) = 4.3563, p = 0.000097; $ES_{(51)}$: t(38) = 4.4428, p = 0.000074; $H'_{(log2)}$: t(38) = 3.3976, p = 0.001607), while evenness (J') was significantly lower in the iron-enriched sediments (t-test: t(38) = 3.720, p = 0.000642), with lower values in the uppermost centimeters and increasing values with increasing sediment depth (Supplement Table S4).

As already described for the bacteria, the NMDS plot also showed a more heterogeneous structure for the nematode community in the sediments from PC1-4. The PC5-8 samples plotted clearly closer together, with the exception of the samples from the deepest sediment layer (PC5-8, 4-5 cm). These samples were markedly dissimilar to those from the upper sediment layers (0-4 cm) and plotted closer to the samples from PC1-4 (Figure 5B).

The SIMPER analysis showed that in the nematode community from the iron-enriched sediments, only two genera already explained 70% of the average similarity within the community (*Thalassomonhystera*: 48% and *Tricoma*: 22%). While in the unaffected sediments ten genera were needed to explain roughly 70% of the similarity within the community (*Thalassomonhystera*: 15%, *Sabatieria*: 12%, *Acantholaimus*: 10%, *Tricoma*: 8%, *Leptolaimus*: 6%, *Halalaimus*: 6%, *Amphimonhystera*: 5%, *Desmoscolex*: 5%, *Amphimonhystrella*: 3%, and *Cervonema*: 3%).

Already at the family level, there were clear differences in the dominance structure of the nematode community from the sediments of the iron-enriched cores (PC1-4) compared to the unaffected sediments (PC5-8). In the sediments of cores PC1-4, three families occurred in a dominance of more than 5%: Desmoscolecidae (39%), Monhysteridae (19%) and Oxystominidae (6%). These three families were also dominant in the sediments from cores PC5-8 (Desmoscolecidae: 25%, Monhysteridae: 16%, Oxystominidae: 5%), but in addition, four more families occurred with a dominance ≥ 5% (Chromadoridae: 9%, Comesomatidae: 13%, Microlaimidae: 6%, Xyalidae: 9%). On genus level, three genera occurred in the iron-enriched sediments with dominance ≥ 5% (*Desmoscolex*: 15%, *Thalassomonhystera*: 17%, *Tricoma*: 25%). In the unaffected sediments six genera dominated the nematode community with ≥ 5% (*Acantholaimus*: 7%, *Desmoscolex*: 5%, *Microlaimus*: 6%, *Sabatieria*: 8%, *Thalassomonhystera*: 13%, *Tricoma*: 18%). A more detailed view of the distribution of the individual genera between iron-enriched and visually unaffected sediments is provided by a heatmap (Table 3).

Members of genera *Desmoscolex*, *Tricoma* and *Thalassomonhystera* also constituted a significant fraction of the community in both iron-enriched and unaffected sediments. Nevertheless, the heat map also showed that the nematodes found in the ferrous sediments were more evenly distributed among a clearly lower number of genera than in the non-ferrous sediments.

Approximately 80% of all nematodes found in both the iron-enriched (81%) and unaffected sediments (79%) belonged to the selective (1a) or non-selective (1b) particle feeding types. The proportion of nematodes described as epigrowth feeders (feeding type 2a) was lower in the iron-enriched sediments (11%) than in the unaffected sediments (18%). Predatory/omnivorous nematodes (feeding type 2b), on the other hand, were more abundant in PC1-4 sediments (8%) than in PC5-8 sediments (3%).

Roughly half of all nematodes (49%) in the ferrous sediments had a c-p value of 4, while in the non-ferrous sediments, approximately half of all nematodes (51%) had a c-p value of 2. The proportion of nematodes with a c-p value of 3 was about the same in the PC1-4 and PC5-8 sediments (14% and 18%, respectively).

10.3389/fmars.2023.1118431

TABLE 2 Bacterial community composition at genus resolution. Heatmap of the dominant community members along the sampled transect. Displayed are average values (%) per push-core, integrating the surface sediment from 0-5 cm depth. Only genera with a minimum relative abundance of 0.1% are shown (all values below 0.1% but above 0.01% still show pale colours). Asterisks indicate significant variance between means of iron-impacted (PC1-4) and unaffected (PC5-8) sediment communities (FDR adjusted p-values: *p>0.05, **p>0.01, ***p>0.001).

	Ferrous sediments				Non-ferrous sediments			
	PC1	PC2	PC3	PC4	PC5	PC6	PC7	PC8
**Lutibacter	0.7	19.6	13.4	14.8	3.3	0	0	0
***Woeseia	3.8	2.7	3.2	3.4	7.4	9.6	9.3	9.7
**Gallionella	20.5	11.5	8.4	3.9	0	0	0	0
**Geopsychrobacter	0	10.2	8.9	8.2	2.3	0.1	0.1	0
Mariprofundus	14.2	1	3.6	1.3	0	0	0	0
***Roseobacter clade NAC11–7 lineage	4.2	3.9	4.4	3.6	0.2	0	0	0.1
Maritimimonas	0.3	1.2	1.9	2	9.7	0	0	0
***o_Actinomarinales	1.1	0.6	1.2	1	2.3	2.4	1.9	2
***Urania–1B–19 marine sediment group	0.5	0.6	1	0.7	1.4	2.4	2.4	2.2
Aquibacter	0.5	1	1.2	2	1	0.8	0.8	0.8
Pir4 lineage	0.5	0.8	1	1.1	1.2	1	1	0.9
**c_Subgroup_21	0.6	0.6	0.8	0.8	1.1	1.2	1.1	1.1
Kordiimonas	0.2	1.8	0.9	1.9	0.9	0.3	0.4	0.4
***Cycloclasticus	1	2.2	0.9	1.8	0.8	0	0	0
**Nitrosomonas	0.2	0.5	0.6	0.7	0.8	0.8	0.8	0.8
***Subgroup 10	0.4	0.2	0.2	0.2	0.7	1.1	0.9	0.9
o_Actinomarinales	0.4	0.5	0.8	0.5	0.6	0.7	0.6	0.5
*Colwellia	2	0.7	0.7	0.5	0.1	0	0.1	0.2
f_Hyphomicrobiaceae	0.8	0.4	0.5	0.5	0.5	0.5	0.5	0.4
***Sulfurospirillum	0.7	1.3	1	1	0	0	0	0
***o_AT–s2–59	0.3	0.2	0.2	0.2	0.6	0.8	0.8	0.8
***Nitrospina	0	0	0.1	0.1	0.6	0.7	1	1
***Sva0996 marine group	0.2	0.2	0.4	0.4	0.5	0.8	0.6	0.5
**o_Kordiimonadales	0	1	0.4	1.9	0.1	0	0	0
***Nitrospira	0.1	0.1	0.1	0.2	0.7	0.8	0.6	0.7
o_Actinomarinales	0.2	0.3	0.4	0.4	0.4	0.6	0.5	0.6
f_PS1_clade	0	1.7	0.6	0.6	0.2	0	0	0
f_Kiloniellaceae	0.3	0.2	0.4	0.3	0.5	0.5	0.4	0.4
***AqS1	0.1	0.1	0.1	0.1	0.6	0.6	0.7	0.8
o_Actinomarinales	0.3	0.2	0.3	0.3	0.4	0.6	0.5	0.4
o_Actinomarinales	0.1	0.1	0.2	0.2	0.3	0.7	0.6	0.8
o_NB1–j	0.1	0.2	0.3	0.3	0.6	0.5	0.4	0.4
***f_Cyclobacteriaceae	0.1	0.1	0.3	0.2	0.5	0.6	0.5	0.4
***Pelagibius	0.1	0.1	0.1	0.1	0.5	0.7	0.6	0.5
*Oleiphilus	1.4	0.6	0.4	0.3	0	0	0	0
Methyloprofundus	2.2	0.2	0.2	0	0	0	0	0
o_Actinomarinales	0.1	0.1	0.2	0.2	0.3	0.6	0.5	0.5
***f_Rhodobacteraceae	0	0.2	0.9	1.3	0	0	0	0
f_Kiloniellaceae	0.2	0.1	0.2	0.2	0.3	0.6	0.4	0.4
***o_AT–s2–59	0.2	0	0.1	0.1	0.4	0.6	0.5	0.4
f_Kiloniellaceae	0.2	0.2	0.2	0.2	0.2	0.4	0.4	0.4
**Blastopirellula	0.1	0.3	0.2	0.3	0.3	0.4	0.4	0.3
f_Kiloniellaceae	0.2	0	0	0	0.2	0.3	0.9	0.6
ET–SHO	0	0.4	0.4	0.7	0.6	0	0	0

The environmental conditions from the nematodes' point of view within the uppermost centimeter in the ferrous (PC1-4) and non-ferrous sediments (PC5-8) were classified from bad to high based on the percentage of c-p classes and the total values for MI, ITD, and H'. Different classifications were found depending on the indicators used (Table 4). The indicators for assessing the environmental conditions did not clearly indicate worse conditions for the nematode community within the ferrous sediments than within the non-ferrous sediments. However, it is striking that all indicators for the sediments from PC1, the push corer taken closest to the iron source and therefore probably containing the highest iron content, showed bad environmental conditions. In addition, most indicators showed worse (in some cases equal) environmental conditions for the sediments in the transition area from ferrous to non-ferrous sediments (PC4) compared to the sediments from all other push cores (apart from PC1). According to the H' values, the environmental quality of the ferrous sediments was ranked from bad to moderate; the environmental quality of the non-ferrous sediments from moderate to good. Based on the ITD, environmental quality could be ranked from bad to good in the ferrous sediments and from moderate to good in the non-ferrous sediments. The classification results based on MI and the percentages of classes c-p 2 and 4 were very consistent (good to high), except for sediments from PC1 (rated as bad). Environmental conditions were assessed as bad to good in the ferrous sediments and poor to moderate in the non-ferrous sediments according to the proportions of the other c-p classes.

10.3389/fmars.2023.1118431

TABLE 3 Nematode community composition at genus resolution. Heatmap of the dominant community members along the sampled transect. Displayed are average abundances for individual taxa per push-core, integrating the surface sediment from 0-5 cm depth. Only genera with a minimum relative abundance of 2% are shown.

	Ferrous sediments				Non-ferrous sediments			
	PC1	PC2	PC3	PC4	PC5	PC6	PC7	PC8
Tricoma	2.5	6.2	5.4	4.4	19.4	8	10.6	19
Thalassomonhystera	3.6	5	4	3.1	9.3	12.2	13.9	13.4
Desmoscolex	0	5.6	4	2.5	10.2	6.2	4	8.4
Acantholaimus	1.8	1.8	1.8	0	7.8	7.1	10.4	9.6
Sabatieria	1.8	1.8	0	0	16.6	5.4	5.4	4.4
Microlaimus	0	3.6	0	0	9.4	1.8	5.4	12
Leptolaimus	1.8	2.5	0	0	8.7	5.9	4.7	6.9
Halalaimus	0	4	0	0	7.8	3.6	6.4	7.6
Campylaimus	1.8	1.8	1.8	1.8	5.6	4.4	5.4	4
Amphimonhystera	0	1.8	2.5	0	5.6	3.6	7.4	3.6
Amphimonhystrella	0	0	0	0	9.1	4.4	5.6	3.1
Monhystrella	0	0	2.5	0	4.4	5	4.7	4.4
Cervonema	0	0	0	0	8.2	4	3.1	5.4
Daptonema	0	0	0	0	5.6	6.9	3.1	3.1
Molgolaimus	0	0	0	0	8.2	1.8	2.5	4.4
Syringolaimus	0	1.8	1.8	0	4	3.6	2.5	3.1
Diplolaimella	0	1.8	0	0	3.6	2.5	3.6	5
Neochromadora	1.8	1.8	0	0	1.8	4.4	4	1.8
Vasostoma	0	0	0	0	8.6	1.8	1.8	3.1
Theristus	0	1.8	0	0	3.1	1.8	4	4
Diplopeltoides	0	0	0	0	4.4	3.1	4	3.1
Sphaerolaimus	0	0	1.8	0	3.6	3.1	2.5	2.5
Wieseria	0	2.5	0	0	3.1	1.8	3.6	1.8
Dichromadora	0	0	0	0	2.5	2.5	5.4	1.8
Camacolaimus	1.8	0	1.8	0	0	1.8	3.1	3.6
unclassified genus	2.5	0	0	1.8	0	1.8	1.8	1.8
Siphonolaimus	0	0	0	0	3.6	0	2.5	3.1
Litinium	0	0	0	0	1.8	1.8	2.5	2.5
Aegialoalaimus	0	0	0	0	2.5	0	2.5	3.6
Diplopeltula	0	0	0	0	4	1.8	2.5	0
Oxystomina	0	0	0	0	3.1	3.1	1.8	0
Metasphaerolaimus	1.8	0	1.8	2.5	0	0	1.8	0
Leptolaimoides	0	0	0	1.8	0	0	2.5	3.1
Desmolaimus	0	0	0	0	1.8	2.5	0	1.8
Southerniella	0	0	0	0	3.1	0	1.8	0
Actinonema	0	0	0	0	0	1.8	0	2.5
Alaimella	0	0	0	0	0	0	1.8	1.8
Anticoma	1.8	0	0	0	0	0	0	1.8
Megadesmolaimus	0	0	0	0	0	1.8	1.8	0
Metalinhomoeus	0	0	0	0	1.8	1.8	0	0
Paramesacanthion	0	0	0	1.8	0	0	1.8	0
Spirinia	0	0	0	0	0	0	0	3.1
Enoplolaimus	0	0	0	0	0	0	0	2.5
Thalassoalaimus	0	0	0	0	0	2.5	0	0

Relation of environmental and food-related variables to bacteria and nematode community structure

RELATE analyses demonstrated a significant relationship between the bacterial community structure (OTUs) and the full set of environmental/food-related variables (Rho = 0.431, p = 0.0004). The relationship between the nematode community structure and the environmental/food-related variables was less strong in comparison but also significant (Rho = 0.274, p = 0.0045). Results from DistLM analysis on the relationship between environmental parameters on nematode community structure (Table 5) revealed that total variation explained by all five explanatory variables (Fe, BN, CHL, AFDW, H2O) was 26%, which was also given as 'Specified solution' (adjusted R^2 =

TABLE 4 Results of the environmental quality assessment within the uppermost centimeter of ferrous (PC1-4) and non-ferrous sediments (PC5-8) according to different nematode community descriptors as quality indicators.

Core	MI	ITD	H′	c-p 2 and 4	c-p 1 + 2	c-p 3-5
PC1	bad	bad	bad	bad	bad	bad
PC2	high	moderate	moderate	high	good	good
PC3	high	good	moderate	high	good	good
PC4	good	moderate	poor	good	poor	poor
PC5	high	moderate	good	high	moderate	moderate
PC6	good	moderate	good	good	poor	poor
PC7	good	good	good	high	moderate	moderate
PC8	high	moderate	moderate	high	moderate	moderate

MI, maturity index; c-p values, colonizers vs. persisters; H', Shannon-Wiener Index (log2), ITD, index of trophic diversity.

0.13). P-values associated with sequential tests to add environmental/food related variables showed that after fitting the first two variables (Fe, p = 0.0276 and bacterial numbers, p = 0.0001) the addition of the remaining three variables (CHL, AFDW, H2O) to the model was not statistically significant. However, when considering each variable alone (i.e., ignoring all other variables), marginal tests showed also a significant p-value for porosity (H2O; p = 0.0402). For the bacterial community the DistLM showed that total variation explained by all four explanatory variables (Fe, CHL, AFDW, H2O) was 32%, which was also given as 'Specified solution' (adjusted R^2 = 0.24). P-values associated with sequential tests were only for the variable Fe statistically significant (p = 0.0001), adding the remaining three variables to the model was statistically not significant. When considering each variable alone, ignoring all other variables, marginal tests showed also a significant p-value for porosity (p = 0.0142).

Marginal test: explained proportion of each parameter alone, ignoring all other parameters. Sequential test: indicates the increase of explained proportion with each parameter added in a combined model (all specified selection procedure with adjusted R^2 selection criterion). Prop: proportion of total variation explained; Prop (cumul.): running cumulative proportion total; $R^2_{adj.}$: adjusted R^2; Fe: iron content; BN: bacterial numbers; CHL: chlorophyll *a*; AFDW: total organic matter measured as ash-free dry-weight of the sediments; H2O: sediment porosity indicated by the water content of the sediments.

DistLM results visualized by dbRDA plots demonstrated for both bacterial (Figure 6) and nematode communities (Figure 7) a clear break between the samples from iron-enriched and unaffected sediments. The first two axes of the dbRDA plots explained 76% of the fitted bacterial and 74% of fitted nematode community variability. Fe was most strongly related to bacterial community structure (23% of total variation in community assemblage structure) and bacterial numbers to nematode community structure (12% of total variation in community assemblage structure).

Discussion

To better assess the changes in the bacterial and meiofaunal communities along the ~1.5 m transect, variations should be assessed in relation to the size of the organisms observed. For a 0.5 mm long nematode, the average distance of 18 cm between two push cores corresponds to a distance of ~750 m for an average human of 1.8 m, while the total length of the push corer transect corresponds to 5-6 km for a human; for typical sediment-dwelling bacteria ~0.1 µm in size, these distances increase to ~3.5 km between push cores and more than 26 km for the entire transect.

These insights should be kept in mind when considering that all organisms in focus of this study have a rather limited operating range within the sediments. In fact, the thick layer of iron deposits and the compacted sediments closest to the iron source (i.e., the corroding bottom-weights) may have further reduced the dispersal ability of the sediment-inhabiting bacteria and meiofauna. Consequently, differences in environmental conditions on the scale of millimeters to meters can strongly influence microbial distribution and function, and may even affect spatial organization on a submillimeter scale (Nunan et al., 2003). Indeed, bacterial communities often exhibit clear biogeographic patterns in their distribution, with many studies reporting significant distance–decay in bacterial community composition (Lear et al., 2014).

For nematodes (and probably also for other meiofauna taxa), local hydrodynamics play a major role in promoting large-scale dispersal, sometimes in the range of several hundred meters (Bell and Sherman, 1980; Thomas and Lana, 2011). Species-specific feeding, body morphology, and mobility/swimming behaviors modulate absolute nematode dispersal ranges on the scale of centimeters or meters (Thomas and Lana, 2011). For example, Jensen (1981) documented a swimming speed of up to 5 cm min^{-1} for one epistrate-feeding nematode genus. These dispersion mechanisms may of course complicate the interpretation of the small-scale distribution patterns of nematodes along the short transect investigated within our study. Yet, our results support our hypothesis that the local input of structural steel at the seabed strongly affects the abundance, distribution, and diversity of the small benthic biota at a sub-meter scale.

Bacterial communities along the iron gradient

The oxidation of iron, likely both abiotically and biotically, created a dense layer of iron deposits that deprived the underlying sediments in PC1-4 of oxygen, creating diverse microbial niches distinct from the ambient fully oxygenated sediments. This

10.3389/fmars.2023.1118431

TABLE 5 DistLM (distance-based linear model) results showing the relationship between environmental (iron content, food availability and sedimentporosity) parameters on variation in nematode and bacteria community structure (Bray-Curtis similarity of square-root transformed abundance ofnematode and bacteria taxa).

Parameter	Pseudo-F.	P.	Prop.	
Marginal				
Bacteria				
Fe	9.8450	0.0001	0.2300	
CHL	1.9560	0.0142	0.0560	
AFDW	1.0080	0.3680	0.0230	
H2O	1.9560	0.0540	0.0770	
Nematoda				
Fe	1.9590	0.0249	0.0560	
BN	4.5880	0.0001	0.1200	
CHL	1.3050	0.2001	0.0380	
AFDW	1.1640	0.2906	0.0340	
H2O	1.8300	0.0402	0.0520	
	Pseudo-F.	P. (cumul.)	Prop. (cumul.)	$R^2_{(adj.)}$ (cumul.)
Sequential				
Bacteria				
Fe	9.8450	0.0001	0.2300	0.2060
CHL	1.8060	0.0606	0.2710	0.2370
AFDW	1.1090	0.2875	0.2970	0.2170
H2O	1.3420	0.1709	0.3280	0.2150
Nematoda				
Fe	1.9590	0.0276	0.0560	0.0270
BN	4.3580	0.0001	0.1690	0.1170
CHL	1.3950	0.1487	0.2050	0.1280
AFDW	1.0900	0.3616	0.2330	0.1310
H2O	0.9660	0.4800	0.2580	0.1300

distinction was most pronounced in the higher relative abundance of Zetaproteobacteria and Campylobacteria in the sediments closest to the iron source. Zetaproteobacteria, here entirely composed of the genus *Mariprofundus* (Supplement Figure S2), are chemolithoautotrophs that couple iron oxidation to oxygen respiration, producing reactive iron oxides that can adsorb or coprecipitate nutrients and metals (Laufer et al., 2017). They are microaerophiles that live in oxic-anoxic transition zones of iron-rich marine habitats, e.g., hydrothermal vents or steel corrosion biofilms (McAllister et al., 2019). Similarly, Campylobacteria, represented here primarily by *Sulfurospirillum* (Supplement Figure S2), are found under microaerophilic to anaerobic conditions often associated with hydrothermal-vent habitats (Campbell et al., 2006). *Sulfurospirillum* members are metabolically diverse, often involved in sulphur and nitrogen cycling. Experimental work also revealed an involvement of *Sulfurospirillum* in iron reduction *via* sulfur cycling, utilizing sulfur or thiosulfate as an electron acceptor (Lohmayer et al., 2014). Other dominant genera involved in iron cycling are the iron oxidizing *Gallionella* and iron reducing *Geopsychrobacter*, both known from low-oxygen habitats (Anderson and Pedersen, 2003), which built up to very high relative abundance in PC1-4, but were mostly absent from PC5-8 (Supplement Figure S2). Interestingly, several of the taxa enriched in iron-affected sediments have been linked to the degradation of different types of hydrocarbons, including *Cycloclasticus*, known for its ability to degrade polycyclic aromatic hydrocarbons (PAHs) (Cui et al., 2008), *Oleiphilus*, growing on aliphatic hydrocarbons, alkanoates and alkanoles (Toshchakov et al., 2017), as well as *Colwellia*, potentially degrading gaseous and aromatic hydrocarbons (Mason et al., 2014). Hydrocarbons, both from natural sources and anthropogenic activities, are thought to accumulate in marine sediments (Duran and Cravo-Laureau, 2016). The higher relative abundance of specialized degraders in the iron-impacted sediments could point towards a chemical interaction between iron oxides and organic matter potentially affecting solubility, bioavailability and composition of carbon sources for microbial degradation (Adhikari and Yang, 2015). The encountered high relative abundances of specialist taxa and chemolithoautotrophs suggest that sunken metal structures can have a significant impact on local microbial community structure and biogeochemistry, and further could serve as stepping stones for the dispersal of specialized microbial consortia in the deep sea, similar to the proposed role of whale or wood falls (Bienhold et al., 2013; Levin et al., 2016; Varliero et al., 2019).

Bacterial communities in the ambient sediments of PC5-8 were characterized by the presence of primarily heterotrophic taxa adapted to periodic and variable input of organic matter from the surface ocean (Jørgensen and Boetius, 2007). Many of these taxa have been reported for various other deep-sea regions (Bienhold et al., 2016), including the genus *Woeseia*, ubiquitous in marine surface sediments around the world (Hoffmann et al., 2020) and among the most abundant taxa in the sediments analyzed here. Members of the *Woeseiaceae* family have been attributed a high metabolic versatility: Genomic analyses of representatives from oxygenated deep-sea sediments suggested a role in the degradation of proteinaceous matter, possibly derived from deposited detrital matter (Hoffmann et al., 2020), but also have indicated a potential for denitrification and chemolithoautotrophic growth *via* sulfur oxidation (Mußmann et al., 2017). The ability to switch from one lifestyle to the other depending on oxygen availability (Buongiorno et al., 2020) may explain their relatively high relative abundance in both iron-affected and ambient sediments. Several other taxa known for their key roles in nitrogen cycling at the seafloor were also significantly more abundant in ambient sediments than in the sediments affected by the iron deposit, including the ammonium oxidizing *Nitrosomonas*, and nitrite oxidizing *Nitrospina* and *Nitrospira* (Zhao et al., 2019), which consume and transform ammonia freed by the mineralization of organic matter.

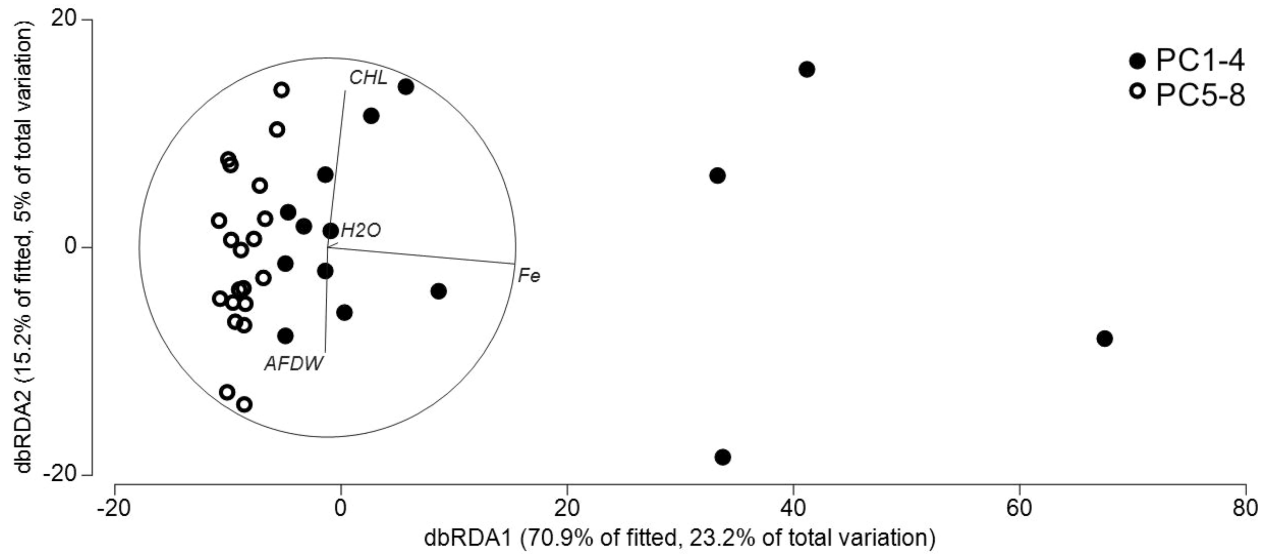

FIGURE 6
Distance-based redundancy analysis ordination to investigate relationship between the environmental variables and bacteria communities in ferrous and non-ferrous sediments. CHL: chlorophyll *a*; AFDW: total organic matter measured as ash-free dry-weight of the sediments; H2O: sediment porosity indicated by the water content of the sediments.

Nematode assemblages along the iron gradient

Tolerance to metal pollutants has been shown to vary widely among nematode species (e.g., Vranken et al., 1991; Kammenga et al., 1994; Moens et al., 2014; Zeppilli et al., 2015). Some species, such as *Enoplus communis*, show low tolerance to metals (Howell, 1983), while others, such as *Diplolaimella dievengatensis* and *Halomonhystera disjuncta* (Vranken and Heip, 1986; Vranken et al., 1991; Gyedu-Ababio and Baird, 2006) can be tolerant to high levels of heavy metals (Zeppilli et al., 2015). Large-scale observations (at hundreds of meters and kilometers) assessing nematode community compositions influenced by multiple metal pollutants have shown that shifting meiobenthic compositions may indicate the presence of metal-tolerant as well as metal-intolerant nematode species (Bastami et al., 2017; Stark et al., 2020).

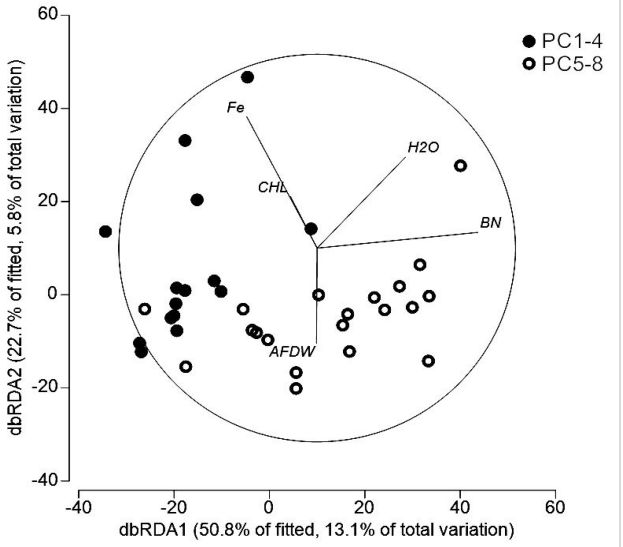

FIGURE 7
Distance-based redundancy analysis ordination to investigate relationship between the environmental variables and nematode communities in ferrous and non-ferrous sediments. CHL: chlorophyll *a*; BN: bacterial numbers; AFDW: total organic matter measured as ash-free dry-weight of the sediments; H2O: sediment porosity indicated by the water content of the sediments.

Generally, studies on how metal pollution affects nematode assemblage composition report lower species diversity and lower abundances of community members (Nasira et al., 2010; Sedano et al., 2014; Bastami et al., 2017; Ridall and Ingels, 2021). This is also evident in the present study: nematode density as well as diversity of the nematode community were significantly lower in the iron-enriched sediments compared to the visually unaffected sediments. In addition, the SIMPER analysis showed a lower within-group similarity for the nematode community from the iron-enriched sediments compared to the unaffected sediments, which was most pronounced in the upper sediment layer (22% in PC1-4, 50% in PC5-8). It seems that the thick layer of iron deposits within the upper sediment layers reduced the dispersal or settling ability of the nematodes from the iron-enriched sediments compared to the unaffected sediments.

Nevertheless, the DistLM approach indicated that the Fe concentration was a stronger predictor of bacteria community structure than of the nematode community structure, with the composition of the nematode community more accurately determined by the number of bacteria; the nematode community thus seems to be influenced more indirectly by the iron concentration *via* its influence on the number of bacteria (see below). Deep-sea nematodes are mainly dominated by deposit feeders, with small buccal cavities which feed selectively (feeding type 1a) or non-selectively (feeding type 1b) on bacteria and other detrital particles (Giere, 2009; Zeppilli et al., 2014). This is also evident in the nematode communities from both iron-enriched and

unaffected sediments. Both communities are dominated by genera belonging to feeding types 1a or 1b.

In general, free-living nematodes are described as the last to disappear from heavily polluted bottom sediments (Heip et al., 1985; Davydkova et al., 2005). High heavy metal resistance in nematodes (Cu, Zn, Pb, Cd, Hg) has been reported (Davydkova et al., 2005 and citations therein), where non-selective deposit-feeders and omnivores seem to be extremely non-sensitive (Davydkova et al., 2005). However, the higher dominance of non-selective deposit feeding nematodes within metal polluted sediments is not confirmed by our results, as the proportion of non-selective deposit feeders in the non-ferrous sediments is clearly higher. In contrast, the comparatively higher proportion of selectively feeding nematodes in the iron-enriched sediments underscores the DistLM result on the importance of bacteria as a potential food source (e.g., compared to phytodetritial matter) for nematode community structure. Selective feeding nematodes, represented here mainly by genera of the Desmoscolecidae, have minute buccal cavities that can only feed on very small (bacterial-sized) prey. Intriguingly, the proportion of genera belonging to feeding type 2b, which is described as predatory and omnivorous, is clearly higher in the iron-enriched sediments (8%) than in the visually unaffected sediments (3%). This becomes particularly clear when considering the uppermost centimeter of the sediments, with the strongest influence of iron (10% vs. 2%).

Interactive relationships in bacteria and nematoda

In deep-sea sediments, bacteria and nematodes dominate benthic biomass and play key roles in nutrient cycling and energy transfer (Rzeznik-Orignac et al., 2018). However, information on the relationships of co-occurring bacterial and nematode communities in deep-sea sediments is rather limited (Ingels et al., 2011). Understanding the biogeochemical and ecological processes that shapes these relationships require insights into local community structures in bacteria and nematodes at very small spatial scales (Rzeznik-Orignac et al., 2018).

As the most numerous and diverse group of deep-sea benthic meiofauna, nematodes usually occupy multiple trophic levels in benthic food webs (Schratzberger et al., 2019) and interact with bacteria to affect carbon metabolic activity (Wu et al., 2019 and citations therein). Diversity patterns of these communities remain poorly studied (Rzeznik-Orignac et al., 2018) and trophic interactions between benthic nematodes and sediment bacteria are generally poorly understood (Viera et al., 2022). In fact, previous work addressing the question of co-occurrence of bacteria and nematodes with quantitative tools came to opposite results: A high number and biomass of meiofauna correlated with a low number and biomass of bacteria in sandy beach sediments in the Kiel Fjord and Kiel Bight (Baltic Sea), and a lack of correlation between meiofauna and bacterial biomass was observed in the deep Aegean, whereas a strong correlation between meiofauna density and the number of viable bacteria was observed in the deep region of the Gulf of Lion (Rzeznik-Orignac et al., 2018 and citations therein). Recent work that focused on ecosystem processes showed correlations between sediment microbiota and nematodes on the slope in the North-western Mediterranean (Román et al., 2019), whereas specific associations between nematodes and bacteria have also been detected in a nearby canyon system (Rzeznik-Orignac et al., 2018).

All these studies showed that ecological interactions between meiofauna and benthic bacteria are generally important for sediment ecology (Rzeznik-Orignac et al., 2018). Meiofauna can promote mineralization of different types of organic matter by stimulating bacterial community activity in the sediment (Nascimento et al., 2012), while higher abundance of meiofauna can reduce microbial mineralization by altering the composition of the bacterial community through grazing (Näslund et al., 2010). In any case, meiofauna such as nematodes have the potential to indirectly influence the activity and/or species composition of microbial communities (De Mesel et al., 2004; Moens et al., 2005).

In the present study, local environmental conditions in the iron-enriched and unaffected sediments differed in terms of physical and geochemical controls on bacterial and thus nematode activity. The oxidation of iron created a dense layer of iron deposits that deprived the underlying sediments by reducing the transfer of phytodetritial organic matter *via* bioturbation to the deeper sediment layers and also by limiting the dispersal ability of the organisms. Our results suggest that the iron-enriched sediments provided a less dynamic environment with comparatively stable/homogeneous conditions (at least at sub-surface sediment layers) that supported a less diverse but more specialized microbial community, represented by a high relative abundance of chemolithoautotrophs. Similarily, the nematode community of the iron-enriched sediments reflected the less dynamic/more stable conditions in a less divers nematode community, more strongly dominated by persisters (cp-value of 4) predominantly belonging to the family Desmoscolecidae compared to the unaffected sediments.

The genera of this nematode family share some morphological/functional features that seem to help them gain a competitive advantage over other nematode genera in the environment of iron-enriched sediments. Their comparably robust bodies allow them to move/migrate even in the more compact sediments of the iron-enriched sediments through burrowing and by creating their own space. Desmoscolecids belong to feeding type 1a, and they can be expected to rely mainly on bacteria as a food source than members of other feeding guilds, as they have minute buccal cavities that can only feed on very small (bacteria-sized) prey. It has been suggested that chemosynthetic bacterial production may constitute an important food source for the benthic organisms that live in partly anoxic sediments (Soetaert et al., 2002a). The expected localized enrichment in chemosynthetic bacterial production in the iron-enriched and most probably subtoxic sediments thus might constitute an additional high-quality food source in the otherwise comparatively food-diluted iron-enriched sediments, giving a competitive edge to the nematode genera/feeding types that have access to this food source (Soetaert et al., 2002b).

Conclusions

Bacterial and nematode communities co-occurring in the sediments along the iron gradient in focus within this study

exhibited spatial distribution patterns that emerged from highly localized community dynamics that were both stochastic and deterministic. The localized input of iron or steel evidently has implications for the ecology of the seafloor by introducing novel niche space and the establishment of specialized communities. Although it was not possible to fully identify the environmental/ecological drivers behind the observed bacterial-nematode associations, our results highlight the importance of small-scale sampling in combination with diversity assessments of different benthic size-compartments for analyzing the variability and potential functions of deep-sea communities. Future research should contextualize benthic community interactions at different trophic levels to gain a deeper understanding of the functional and structural characteristics of benthic communities.

Data availability statement

The datasets presented in this study can be found in online repositories. The names of the repository/repositories and accession number(s) can be found in the Supplementary Material.

Author contributions

TS, JR: conceived the study. JR, CH: did the statistical analyses. TS, JR, CH: wrote the paper. All authors contributed to the article and approved the submitted version.

Funding

This research has been supported by the Alfred Wegener Institute Helmholtz Centre for Polar and Marine Research, AWI (Grant no. AWI_PS108_00). JR received support through the European Research Council Advanced Investigator grant 294757 (Antje Boetius).

Acknowledgments

We would like to thank the officers and crew of our RV *Polarstern* expedition PS93.2 in 2015, as well as the team operating the MARUM ROV *QUEST 4000*. Dr. Susann Henkel and Ingrid Stimac from the AWI section "Marine Geochemistry" are gratefully acknowledged for the analysis of the iron contents of the sediments. We thank Anja Pappert, Jakob Barz, and Erik Dauer for their assistance with the measurements of various sediment parameters, DNA extractions, bacteria counting, meiofauna sorting, and the preparation of slides for nematode identification. We also gratefully acknowledge two reviewers for their valuable comments on the manuscript.

Conflict of interest

The authors declare that the research was conducted in the absence of any commercial or financial relationships that could be construed as a potential conflict of interest.

Publisher's note

All claims expressed in this article are solely those of the authors and do not necessarily represent those of their affiliated organizations, or those of the publisher, the editors and the reviewers. Any product that may be evaluated in this article, or claim that may be made by its manufacturer, is not guaranteed or endorsed by the publisher.

Supplementary material

The Supplementary Material for this article can be found online at: https://www.frontiersin.org/articles/10.3389/fmars.2023.1118431/full#supplementary-material

References

Adhikari, D., and Yang, Y. (2015). Selective stabilization of aliphatic organic carbon by iron oxide. *Sci. Rep.* 5, 11214. doi: 10.1038/srep11214

Alfred-Wegener-Institut Helmholtz-Zentrum für Polar- und Meeresforschung (2017). Polar research and supply vessel POLARSTERN operated by the Alfred-Wegener-Institute. *J. large-scale Res. facilities* 3, A119. doi: 10.17815/jlsrf-3-163

Allianz Global Corporate & Specialty (2022). AGCS safety & shipping review. *Annu. Rep.*, 66.

Andersen, K. S., Kirkegaard, R. H., Karst, S. M., and Albertsen, M. (2018). ampvis2: an r package to analyse and visualise 16S rRNA amplicon data. *bioRxiv*, 299537. doi: 10.1101/299537

Anderson, M. J., Gorley, R. N., and Clarke, K. R. (2008). *PERMANOVA+ for PRIMER: guide to software and statistical methods* (UK: PRIMER-E, Plymouth).

Anderson, C. R., and Pedersen, K. (2003). *In situ* growth of *Gallionella* biofilms and partitioning of lanthanides and actinides between biological material and ferric oxyhydroxides. *Geobiol* 1 (2), 169–178. doi: 10.1046/J.1472-4669.2003.00013.X

Andrassy, I. (1956). The determination of volume and weight of nematodes. *Acta Zool. Acad. Sci. Hungary* 2 (1-3), 1–15.

Andrews, S. (2010) *FastQC: a quality control tool for high throughput sequence data*. Available at: http://www.bioinformatics.babraham.ac.uk/projects/fastqc/.

Børsheim, K. Y., Bratbak, G., and Heldal, M. (1990). Enumeration and biomass estimation of planktonic bacteria and viruses by transmission electron microscopy. *Appl. Environ. Microbiol.* 56, 352–356. doi: 10.1128/aem.56.2.352-356.1990

Bastami, K. D., Taheri, M., Foshtomi, M. Y., Haghparast, S., Hamzehpour, A., Bagheri, H., et al. (2017). Nematode community structure in relation to metals in the southern of Caspian Sea. *Acta Oceanol Sin.* 36, 79–86. doi: 10.1007/s13131-017-1051-x

Bell, S. S., and Sherman, K. (1980). A field investigation of meiofaunal dispersal: tidal resuspension and implications. *S Mar. Ecol. Prog. Ser.* 3, 245–249. doi: 10.3354/meps003245

Benjamini, Y., and Hochberg, Y. (1995). Controlling the false discovery rate: A practical and powerful approach to multiple testing. *J. R. Stat. Soc Ser. B* 57, 289–300. doi: 10.2307/2346101

Bienhold, C., Pop Ristova, P., Wenzhöfer, F., Dittmar, T., and Boetius, A. (2013). How deep-Sea wood falls sustain chemosynthetic life. *PloS One* 8, e53590. doi: 10.1371/journal.pone.0053590

Bienhold, C., Zinger, L., Boetius, A., and Ramette, A. (2016). Diversity and biogeography of bathyal and abyssal seafloor bacteria. *PloS One* 11, e0148016. doi: 10.1371/journal.pone.0148016

Bolger, A. M., Lohse, M., and Usadel, B. (2014). Trimmomatic: A flexible trimmer for illumina sequence data. *Bioinformatics* 30, 2114–2120. doi: 10.1093/bioinformatics/btu170

Bongers, T. (1990). The maturity index: An ecological measure of environmental disturbance based on nematode species composition. *Oecologia* 83, 14–19. doi: 10.1007/BF00324627

Bongers, T., Alkemade, R., and Yeates, G. W. (1991). Interpretation of disturbance-induced maturity decrease in marine nematode assemblages by means of the maturity index. *Mar. Ecol. Prog. Ser.* 76, 135–142. doi: 10.3354/meps076135

Bongers, T., and Bongers, M. (1998). Functional diversity of nematodes. *Appl. Soil Ecol.* 10, 239251. doi: 10.1016/S0929-1393(98)00123-1

Bongers, T., de Goede, R. G. N., Korthals, G. W., and Yeates, G. W. (1995). Proposed changes of c-p classification for nematodes. *Russ. J. Nematol* 3 (1), 61–62. doi: 10.1007/BF00324627

Bongers, T., and Ferris, H. (1999). Nematode community structure as a bioindicator in environmental monitoring. *Trends Ecol. Evol.* 14, 224–228. doi: 10.1016/S0169-5347(98)01583-3

Buhl-Mortensen, L., Vanreusel, A., Gooday, A. J., Levin, L. A., Priede, I. G., Buhl-Mortensen, P., et al. (2010). Biological structures as a source of habitat heterogeneity and biodiversity on the deep ocean margins. *Mar. Ecol.* 31, 21–50. doi: 10.1111/j.1439-0485.2010.00359.x

Buongiorno, J., Sipes, K., Wasmund, K., Loy, A., and Lloyd, K. (2020). Woeseiales transcriptional response to shallow burial in Arctic fjord surface sediment. *G PloS One* 15 (8), e0234839. doi: 10.1371/JOURNAL.PONE.0234839

Campbell, B. J., Engel, A. S., Porter, M. L., and Takai, K. (2006). The versatile ϵ-proteobacteria: key players in sulphidic habitats. *Nat. Rev. Microbiol.* 4, 458–468. doi: 10.1038/nrmicro1414

Castaneda, H., and Benetton, X. (2008). SRB-biofilm influence in active corrosion sites formed at steel-electrolyte interface when exposed to artificial seawater conditions. *D Corr Sci.* 50, 1169–1183. doi: 10.1016/j.corsci.2007.11.032

Clarke, K. R., and Gorley, R. N. (2015). *PRIMER v7: User Manual/Tutorial* (UK: PRIMER-E, Plymouth).

Clarke, K. R., Gorley, R. N., Somerfield, P. J., and Warwick, R. M. (2014). *Change in marine communities: an approach to statistical analysis and interpretation. 3rd ed* (UK: PRIMER-E, Plymouth).

Core Team, R. (2017) *R: A language and environment for statistical computing*. Available at: https://www.R-project.org.

Cui, Z., Lai, Q., Dong, C., and Shao, Z. (2008). Biodiversity of polycyclic aromatic hydrocarbon-degrading bacteria from deep-sea sediments of the middle Atlantic ridge. *Env Microbiol.* 10 (8), 2138–2149. doi: 10.1111/J.1462-2920.2008.01637.X

Davydkova, I. L., Fadeeva, N. P., Kovekovdova, L. T., and Fadeev, V. I. (2005). Heavy metal contents in tissue of dominant species of the benthos and in bottom sediments of zolotoi rog bay, Sea of Japan. *Russ. J. Mar. Biol.* 31 (3), 149–180. doi: 10.1007/s11179-005-0064-z

De Grisse, A. T. (1969). Redescription ou modification de quelques techniques utilisées dans l'étude de nematodes phytoparasitires. *Meded Rijsfakulteit Landbouwneten-scheppen Gent* 34, 351–369.

De Mesel, I., Derycke, S., Moens, T., van der Grucht, K., Vincx, M., and Swings, S. (2004). Top-down impact of bacterivorous nematodes on the bacterial community structure: A microcosm study. *Environ. Microbiol.* 6, 733–744. doi: 10.1111/j.1462-2920.2004.00610.x

Duran, R., and Cravo-Laureau, C. (2016). Role of environmental factors and microorganisms in determining the fate of polycyclic aromatic hydrocarbons in the marine environment. *FEMS Microbiol. Rev.* 40 (6), 814–830. doi: 10.1093/femsre/fuw031

Giere, O. (2009). "Meiobenthology," in *The microscopic motile fauna of aquatic sediments* (Heidelberg: Springer-Verlag), 527.

Gobet, A., Boetius, A., and Ramette, A. (2014). Ecological coherence of diversity patterns derived from classical fingerprinting and next generation sequencing techniques. *Environ. Microbiol.* 16, 2672–2681. doi: 10.1111/1462-2920.12308

Grossmann, S., and Reichardt, W. (1991). Impact of *Arenicola marina* on bacteria in intertidal sediments. *Mar. Ecol. Prog. Ser.* 77, 85–93. doi: 10.3354/meps077085

Gyedu-Ababio, T. K., and Baird, D. (2006). Response of meiofauna and nematode communities to increased levels of contaminants in a laboratory microcosm experiment. *Ecotox Environ. Saf.* 63 (3), 443–450. doi: 10.1016/j.ecoenv.2005.01.010

Heip, C., Vincx, M., and Vranken, G. (1985). The ecology of marine nematodes. oceanogr. *Mar. Biol. Annu. Rev.* 23, 399–489.

Hoffmann, K., Bienhold, C., Buttigieg, P. L., Knittel, K., Laso-Pérez, R., Rapp, J. Z., et al. (2020). Diversity and metabolism of woeseiales bacteria, global members of marine sediment communities. *ISME J.* 14, 1042–1056. doi: 10.1038/s41396-020-0588-4

Howell, A. (1983). Heavy metals in marine nematodes: Uptake, tissue distribution and loss of copper and zinc. *Mar. Poll Bull.* 14 (7), 263–268. doi: 10.1016/0025-326X(83)90170-4

Hua, E., Zhu, Y., Huang, D., and Liu, X. (2021). Are free-living nematodes effective environmental quality indicators? insights from bohai bay, China. *Ecol. Ind.* 127, 107756. doi: 10.1016/j.ecolind.2021.107756

Hurlbert, S. H. (1971). The non-concept of species diversity: A critique and alternative parameters. *Ecology* 52 (4), 577–586. doi: 10.2307/1934145

Ingels, J., Billett, D. S. M., Van Gaever, S., and Vanreusel, A. (2011). An insight into the feeding ecology of deep-sea canyon nematodes - results from field observations and the first *in-situ* ^{13}C feeding experiment in the nazaré canyon. *J. Exp. Mar. Biol.* 396 (2), 185–193. doi: 10.1016/j.jembe.2010.10.018

Jørgensen, B. B., and Boetius, A. (2007). Feast and famine - microbial life in the deep-sea bed. *Nat. Rev. Microbiol.* 5 (10), 770–781. doi: 10.1038/nrmicro1745

Jensen, P. (1981). Phyto-chemical sensitivity and swimming behaviour of the free-living marine nematode *Chromadorita tenuis*. *Mar. Ecol. Prog. Ser.* 4, 203–206. doi: 10.3354/meps004203

Kammenga, J. E. C., Van Gestel, A. M., and Bakker, J. (1994). Patterns of sensitivity to cadmium and pentachlorophenol among nematode species from different taxonomic and ecological groups. *Arch. Environ. Contam Toxicol.* 27, 88–94. doi: 10.1007/BF00203892

Kip, N., and Veen, J. A. V. (2015). The dual role of microbes in corrosion. *ISME J.* 9, 542–551. doi: 10.1038/ismej,2014.169

Klindworth, A., Pruesse, E., Schweer, T., Peplies, J., Quast, C., Horn, M., et al. (2013). Evaluation of general 16S ribosomal RNA gene PCR primers for classical and next-generation sequencing-based diversity studies. *Nucleic Acids Res.* 41, e1. doi: 10.1093/nar/gks808

Kuroda, T., Takai, R., Kobayashi, Y., Tanaka, Y., and Hara, S. (2008). "Corrosion rate of shipwreck structural steels under the sea," in *OCEANS 2008 - MTS/IEEE Kobe Techno-Ocean, Kobe*. 1–6. doi: 10.1109/OCEANSKOBE.2008.4531052

Laufer, K., Nordhoff, M., Halama, M., Martinez, R. E., Obst, M., Nowak, M., et al. (2017). Microaerophilic Fe(II)-oxidizing zetaproteobacteria isolated from low-fe marine coastal sediments: Physiology and composition of their twisted stalks. *Appl. Environ. Microbiol.* 83, e03118-16. doi: 10.1128/AEM.03118-16

Lear, G., Bellamy, J., Case, B., Lee, J. E., and Buckley, H. L. (2014). Fine-scale spatial patterns in bacterial community composition and function within freshwater ponds. *ISME J.* 8, 1715–1726. doi: 10.1038/ismej.2014.21

Levin, L. A., Baco, A. R., Bowden, D. A., Colaco, A., Cordes, E. E., Cunha, M. R., et al. (2016). Hydrothermal vents and methane seeps: Rethinking the sphere of influence. *Front. Mar. Sci.* 3. doi: 10.3389/fmars.2016.00072

Lohmayer, R., Kappler, A., Lösekann-Behrens, T., and Planer-Friedrich, B. (2014). Sulfur species as redox partners and electron shuttles for ferrihydrite reduction by *Sulfurospirillum deleyianum*. *Appl. Environ. Microbiol.* 80, 3141–3149. doi: 10.1128/AEM.04220-13

Mahé, F., Rognes, T., Quince, C., de Vargas, C., and Dunthorn, M. (2015). Swarm v2: highly-scalable and high-resolution amplicon clustering. *PeerJ* 3, e1420. doi: 10.7717/peerj.1420

Martin, M. (2011). Cutadapt removes adapter sequences from high-throughput sequencing reads. *EMBnet.journal* 17, 10. doi: 10.14806/ej.17.1.200

Mason, O. U., Han, J., Woyke, T., and Jansson, J. K. (2014). Single-cell genomics reveals features of a *Colwellia* species that was dominant during the deepwater horizon oil spill. *Front. Microbiol.* 5. doi: 10.3389/FMICB.2014.00332

McAllister, S. M., Moore, R. M., Gartman, A., Luther, G. W., Emerson, D., and Chan, C. S. (2019). The Fe(II)-oxidizing zetaproteobacteria: Historical, ecological and genomic perspectives. *FEMS Microbiol. Ecol.* 95, 1-18. doi: 10.1093/femsec/fiz015

McArdle, B. H., and Anderson, M. J. (2001). Fitting multivariate models to community data: A comment on distance-based redundancy analysis. *Ecol* 82, 290–297. doi: 10.1890/0012-9658(2001)082[0290:FMMTCD]2.0.CO;2

Melchers, R. E. (2019). Predicting long-term corrosion of metal alloys in physical infrastructure. *NPJ Mater. Degrad* 3, 1-7. doi: 10.1038/s41529-018-0066-x

Meyer-Reil, L.-A. (1983). Benthic response to sedimentation events during autumn to spring at a shallow water station in the western Kiel bight. *Mar. Biol.* 77, 247–256. doi: 10.1007/BF00395813

Meyer, K. S., Young, C. M., Sweetman, A. K., Taylor, J., Soltwedel, T., and Bergmann, M. (2016). Rocky islands in a sea of mud: biotic and abiotic factors structuring deep-sea dropstone communities. *Mar. Ecol. Prog. Ser.* 556, 45–57. doi: 10.3354/meps11822

Moens, T., Braeckman, U., Derycke, S., Fonseca, G., Gallucci, F., Ingels, J., et al. (2014). "Ecology of free-living marine nematodes," in *Handbook of zoology: Gastrotricha, cycloneuralia and gnathifera*, vol. 2 . Ed. A. Schmidt-Rhaesa (Berlin, Germany: De Gruyter: Nematoda), 109–152. doi: 10.1515/9783110274257.109

Moens, T., Dos Santos, G. A. P., Thompson, F., Swings, J., Fomseca-Genevois, V., Vincx, M., et al. (2005). Do nematode mucus secretions affect bacterial growth? *Aquat Microb. Ecol.* 40, 77–83. doi: 10.3354/ame040077

Moore, J. D.III (2015). Long-term corrosion processes of iron and steel shipwrecks in the marine environment: A review of current knowledge. *J. Mar. Arch.* 10 (3), 191–204. doi: 10.1007/s11457-015-9148-x

Moreno, M., Semprucci, F., Vezzulli, L., Balsamo, M., Fabiano, M., and Albertelli, G. (2011). The use of nematodes in assessing ecological quality status in the Mediterranean coastal ecosystems. *Ecol. Ind.* 11, 328–336. doi: 10.1016/j.ecolind.2010.05.011

Mußmann, M., Pjevac, P., Krüger, K., and Dyksma, S. (2017). Genomic repertoire of the Woeseiaceae/JTB255, cosmopolitan and abundant core members of microbial communities in marine sediments. *ISME J.* 11 (5), 1276–1281. doi: 1038/ismej.2016.185

Nascimento, F. J. A., Näslund, J., and Elmgren, R. (2012). Meiofauna enhances organic matter mineralization in soft sediment ecosystems. *Limnol Oceanogr* 57 (1), 338–346. doi: 10.4319/lo.2012.57.1.0338

Nasira, K., Shahina, F., and Kamran, M. (2010). Response of free-living nematode communities to heavy metal contamination along the coastal areas of sindh and balochistan, Pakistan. *Pak. J. Nematol* 28 (2), 263–278.

Näslund, J., Nascimento, F. J., and Gunnarsson, J. S. (2010). Meiofauna reduces bacterial mineralization of naphthalene in marine sediment. *ISME J.* 4 (11), 1421–1430. doi: 10.1038/ismej.2010.63

Nöthen, K., and Kasten, S. (2011). Reconstructing changes in seep activity by means of pore water and solid phase Sr/Ca and Mg/Ca ratios in pockmark sediments of the northern Congo fan. *Mar. Geol.* 287, 1–13. doi: 10.1016/j.margeo.2011.06.008

Nunan, N., Wu, K., Young, I. M., Crawford, J. W., and Ritz, K. (2003). Spatial distribution of bacterial communities and their relationships with the micro-architecture of soil. FEMS microbiol. *Ecol* 44 (2), 203–215. doi: 10.1016/S0168-6496(03)00027-8

Oksanen, J., Blanchet, F. G., Friendly, M., Kindt, R., Legendre, P., McGlinn, D., et al. (2019). Vegan: Community ecology package. *R package version 2.5-6*. https://CRAN.R-project.org/package=vegan

Pfannkuche, O., and Thiel, H. (1988). "Sample processing," in *Introduction to the study of meiofauna*. Eds. R. P. Higgins and H. Thiel (Washington D.C., London: Smithsonian Institute Press), 134–145.

Pielou, E. C. (1969). *An introduction to mathematical ecology* (New York: Wiley-Interscience).

Quast, C., Pruesse, E., Yilmaz, P., Gerken, J., Schweer, T., Yarza, P., Glöckner, F., et al. (2013).The SILVA ribosomal RNA gene database project: Improved data processing and web-based tools. *O Nucleic Acids Res.* 41, D590–D596. doi: 10.1093/nar/gks1219

Ridall, A., and Ingels, J. (2021). Suitability of free-living marine nematodes as bioindicators: status and future considerations. *Front. Mar. Sci.* 8. doi: 10.3389/fmars.2021.685327

Román, S., Ortiz-Álvarez, R., Romano, C., Casamayor, E. O., and Martin, D. (2019). Microbial community structure and functionality in the deep-Sea floor: Evaluating the causes of spatial heterogeneity in a submarine canyon system (NW Mediterranean, Spain). *Front. Mar. Sci.* 6. doi: 10.3389/fmars.2019.00108

Rzeznik-Orignac, J., Puisay, A., Derelle, E., Peru, E., Le Bris, N., and Galand, P. E. (2018). Co-Occuring nematodes and bacteria in submarine canyon sediments. *PeerJ* 6, e5396. doi: 10.7717/peerj.5396

Schmidt-Rhaesa, A. (2014). "Handbook of zoology," in *Gastrotricha, cycloneuralia and gnathifera*, vol. 2. (Berlin: De Gruyter).

Schratzberger, M., Holtermann, M., van Oevelen, D., and Helder, J. (2019). A worm's world: Ecological flexibility pays off for free-living nematodes in sediments and soils. *BioScience* 69, 867–876. doi: 10.1093/biosci/biz086

Sedano, F., Marquina, D., and Espinosa Torre, F. (2014). Usefulness of meiofauna at high taxonomic levels as a tool to assess harbor quality status. Marina del este harbor (Granada, Spain) as a case study. *Rev. Mar. Cost* 6, 103–113. doi: 10.15359/revmar.6.7

Semprucci, F., Balsamo, M., and Frontalini, F. (2014a). The nematode assemblage of a coastal lagoon (Lake varano, southern italy): ecology and biodiversity patterns. *Sci. Mar.* 78, 579–588. doi: 10.3989/scimar.04018.02A

Semprucci, F., Colantoni, P., Sbrocca, C., Baldelli, G., and Balsamo, M. (2014b). Spatial patterns of distribution of meiofaunal and nematode assemblages in the huvadhoo lagoon (Maledives Indian ocean). *J. Mar. Biol. Assoc. UK* 94, 1377–1385. doi: 10.1017/S002531541400068X

Shannon, C. E., and Weaver, W. W. (1963). "The mathematical theory of communications," *The mathematical theory of communications* (Urbana: University of Illinois Press), 117.

Shuman, F. R., and Lorenzen, C. F. (1975). Quantitative degradation of chlorophyll by a marine herbivore. *Limnol Oceanogr* 20, 580–586. doi: 10.4319/lo.1975.20.4.0580

Soetaert, K., and Heip, C. (1995). Nematode assemblages of deep-sea and shelf break sites in the north Atlantic and Mediterranean Sea. *Mar. Ecol. Prog. Ser.* 123 (1-3), 171–183. doi: 10.3354/meps125171

Soetaert, K., Middelburg, J., Wijsman, J., Herman, P., and Heip, C. (2002a). "Ocean margin early diagenetic processes and models," in *Ocean margin systems*. Eds. G. Wefer, D. Billett, D. Hebbeln, B. B. Jørgensen, v. Weesing and J. T. (Berlin: Springer Verlag), 157–177.

Soetaert, K., Muthumbi, A. W. N., and Heip, C. H. R. (2002b). Size and shape of ocean margin nematodes: morphological diversity and depth related patterns. *Mar. Ecol. Prog. Ser.* 242, 179–193. doi: 10.3354/meps242179

Soltwedel, T., Bauerfeind, E., Bergmann, M., Bracher, A., Budaeva, N., Busch, K., et al. (2016). Natural variability or anthropogenically-induced variation? insights from 15 years of multidisciplinary observations at the arctic marine LTER site HAUSGARTEN. *Ecol. Ind.* 65, 89–102. doi: 10.1016/j.ecolind.2015.10.001

Stark, J. S., Mohammad, M., McMinn, A., and Ingels, J. (2020). Diversity, abundance, spatial variation, and human impacts in marine meiobenthic nematode and copepod communities at Casey station, East Antarctica. *Front. Mar. Sci.* 7. doi: 10.3389/fmars.2020.0048

Taylor, J. R., DeVogelaere, A. P., Burton, E. J., Frey, O., Lundsten, L., Kuhnz, L. A., et al. (2014). Deep-sea faunal communities associated with a lost intermodal shipping container in the Monterey bay national marine sanctuary, CA. *Mar. Poll Bull.* 83, 92–106. doi: 10.1016/j.marpolbul.2014.04.014

Tengberg, A., De Bovee, F., Hall, P., Berelson, W., Chadwick, D., Ciceri, G., et al. (1995). Benthic chamber and profiling landers in oceanography - a review of design, technical solutions and functioning. *Prog. Oceanogr* 35, 253–294. doi: 10.1016/0079-6611(95)00009-6

Thiel, H. (1978). "Benthos in upwelling regions," in *Upwelling ecosystems*. Eds. R. Boje and M. Tomczak (Berlin: Springer Verlag), 124–138.

Thomas, M. C., and Lana, P. C. (2011). A new look into small-scale dispersal of free-living marine nematodes. *Zoologia* 28 (4), 449–456. doi: 10.1590/S1984-46702011000400006

TIBCO Statistica, Inc (2017) *TIBCO statistica (Data analysis software system)*. Available at: https://www.tibco.com.

Toshchakov, S., Korzhenkov, A. A., Chernikova, T. N., Ferrer, M., Golyshina, O. V., Yakimov, M. M., et al. (2017). The genome analysis of *Oleiphilus messinensis* ME102 (DSM 13489T) reveals backgrounds of its obligate alkane-devouring marine lifestyle. *Mar. Genom.* 36, 41. doi: 10.1016/J.MARGEN.2017.07.005

Varliero, G., Bienhold, C., Schmid, F., Boetius, A., and Molari, M. (2019). Microbial diversity and connectivity in deep-sea sediments of the south Atlantic polar front. *Front. Microbiol.* 10. doi: 10.3389/fmicb.2019.00665

Viera, S., Scrozyńska, K., Neves, J., Martins, M., Costa, M. H., Adao, H., et al. (2022). Spatial distribution patterns of microbiome and nematodes in response to sediment ecological conditions. *Microbiol. Ecol. under Rev.* doi: 10.21203/rs.3.rs-1525374/v1. [Accessed November 15, 2022].

Volz, J. B., Liu, B., Köster, M., Henkel, S., Koschinsky, A., and Kasten, S. (2020). Post-depositional manganese mobilization during the last glacial period in sediments of the eastern clarion-clipperton zone, pacific ocean. *Earth Planet Sc Lett.* 532, 116012. doi: 10.1016/j.epsl.2019.116012

Vranken, G., and Heip, C. (1986). Toxicity of copper, mercury and lead to a marine nematode. *Mar. Poll Bull.* 17, 453–457. doi: 10.1016/0025-326X(86)90834-9

Vranken, G., Vanderhaeghen, R., and Heip, C. (1991). Effects of pollutants on life-history parameters of the marine nematode *Monhystera disjuncta*. *ICES J. Mar. Sci.* 48, 325–334. doi: 10.1093/icesjms/48.3.325

Wickham, H. (2016). *ggplot2: Elegant graphics for data analysis* (Springer-Verlag New York). https://ggplot2.tidyverse.org

Wieser, W. (1953). Die beziehung zwischen mundhöhlengestalt, ernährungsweise und vorkommen bei freilebenden marinen nematoden. *Arkiv för Zoologi* 4, 439–484.

Wieser, W. (1960). Benthic studies in buzzards bay. II. the meiofauna. *Limnol Oceanogr* 5, 121–137. doi: 10.4319/lo.1960.5.2.0121

WSC, World Shipping Council (2022). *Containers lost at Sea* (Washington, USA: World Shipping Council). 6.

Wu, X. (2019). *Drivers of nematode community structure and of nematode microbiomes on an estuarine intertidal flat* (Ghent, Belgium: Ghent University. Faculty of Sciences), 206.

Zeppilli, D., Bongiorni, L., Serraõ Santos, R., and Vanreusel, A. (2014). Changes in nematode communities in different physiographic sites of the condor seamount (North-East Atlantic ocean) and adjacent sediments. *PloS One* 9 (12), e115601. doi: 10.1371/journal.pone.0115601

Zeppilli, D., Sarrazin, J., Leduc, D., Arbizu, P. M., Fontaneto, D., Fontanier, C., et al. (2015). Is the meiofauna a good indicator for climate change and anthropogenic impacts? *Mar. Biodiv* 45, 505–535. doi: 10.1007/s12526-015-0359-z

Zhang, J., Kobert, K., Flouri, T., and Stamatakis, A. (2014). PEAR: a fast and accurate illumina paired-end reAd mergeR. *Bioinformatics* 30, 614–620. doi: 10.1093/bioinformatics/btt593

Zhao, R., Hannisdal, B., Mogollon, J. M., and Jørgensen, S. L. (2019). Nitrifier abundance and diversity peak at deep redox transition zones. *Sci. Rep.* 9 (1), 1–12. doi: 10.1038/s41598-019-44585-6

Impact of Local Iron Enrichment on the Small Benthic Biota in the deep Arctic Ocean

Thomas Soltwedel[1*], Josephine Z. Rapp[1,2], Christiane Hasemann[1]

[1] Deep-Sea Ecology and Technology, Alfred-Wegener-Institute Helmholtz-Center for Polar and Marine Research, Am Handelshafen 12, 27570 Bremerhaven, Germany,
[2] Present address : Department of Biochemistry, Microbiology and Bioinformatics, Université Laval, Quebec, QC, Canada

Supplementary Material

1 Tables

Table S1 Overview on samples for bacterial molecular analyses and the generated sequencing output.

Core ID	Depth (cm)	Raw reads	Quality controlled (QC) reads	Reads remaining after QC %	Merged reads	QC reads remaining after merging %
PC1	1	86,492	26,852	31	15,421	57
PC1	2	106,219	29,879	28	18,929	63
PC1	3	129,651	36,551	28	23,185	63
PC1	4	98,208	28,152	29	17,301	61
PC1	5	181,675	52,199	29	32,304	62
PC2	1	92,416	27,642	30	16,384	59
PC2	2	191,300	61,975	32	39,811	64
PC2	3	143,250	44,059	31	28,384	64
PC2	4	142,511	44,934	32	28,258	63
PC2	5	126,783	39,037	31	24,815	64
PC3	1	163,049	49,256	30	30,380	62
PC3	2	120,071	38,253	32	24,513	64
PC3	3	125,089	39,651	32	25,139	63
PC3	4	121,029	38,874	32	24,338	63
PC3	5	130,013	39,794	31	24,909	63
PC4	1	140,453	46,112	33	29,970	65
PC4	2	202,881	65,268	32	43,400	66
PC4	3	144,429	44,387	31	27,249	61
PC4	4	146,680	46,287	32	29,547	64
PC4	5	124,742	39,302	32	25,134	64
PC5	1	136,979	46,054	34	28,134	61
PC5	2	142,086	47,308	33	29,386	62
PC5	3	122,830	40,578	33	24,669	61
PC5	4	135,021	44,005	33	27,778	63
PC5	5	122,449	39,438	32	24,018	61
PC6	1	121,482	41,077	34	25,019	61
PC6	2	113,300	38,290	34	23,158	60
PC6	3	109,923	37,443	34	21,976	59
PC6	4	109,789	37,184	34	22,312	60
PC6	5	101,982	34,332	34	19,848	58
PC7	1	135,865	46,154	34	27,672	60
PC7	2	91,502	30,902	34	18,530	60
PC7	3	126,372	43,068	34	25,815	60
PC7	4	157,237	52,809	34	32,073	61
PC7	5	149,681	50,375	34	30,063	60
PC8	1	116,842	39,678	34	23,947	60
PC8	2	186,630	58,179	31	33,187	57
PC8	3	105,785	33,637	32	19,648	58
PC8	4	93,824	29,727	32	17,131	58
PC8	5	107,233	34,712	32	20,384	59

Table S2 Environmental, bacterial and faunal data in the uppermost 5 cm of the sediments along the iron gradient (Fe: iron concentrations; H2O: water contents; AFDW: ash-free dry-weights; CHL: chlorophyll *a* concentrations; CPE: chloroplastic pigment equivalents; BN: bacterial numbers; BB: bacterial biomass; NEMA: Nematoda densities; NB: Nematoda biomass (wet weight); FORAM: Foraminifera densities; OTHERS: densities of all other metazoan meiofauna; TMEIO: total meiofauna densities).

Core ID	Depth (cm)	Fe (mg g^{-1})	H2O (%)	AFDW (µg)	CHL (µg)	CPE (µg)	BN (cells x 10^8)	BB (µg C cm^{-3})	NEMA (ind. 10^{-2})	NB (µg 10 cm^{-2})	FORAM (ind. 10^{-2})	OTHERS (ind. 10^{-2})	TMEIO (ind. 10^{-2})
PC1	1	n.d.	60.2	246.2	0.18	2.27	0.61	22.04	16	0.67	35	6	57
PC1	2	n.d.	68.7	210.2	0.29	3.72	0.52	20.59	19	0.86	73	0	92
PC1	3	n.d.	52.9	150.4	0.30	6.95	0.51	12.93	10	0.33	41	0	51
PC1	4	n.d.	49.8	212.0	0.46	9.18	0.40	6.93	10	91.26	3	0	13
PC1	5	n.d.	48.7	171.6	0.62	6.67	0.69	15.99	10	18.25	10	0	19
PC1	0-5	n.d.	56.1	990.4	1.85	28.79	2.74	78.46	64	111.37	162	6	232
PC2	1	227.7	65.0	124.6	0.54	6.78	1.35	37.97	57	16.65	146	16	219
PC2	2	114.7	51.4	100.6	0.70	9.83	0.83	21.72	41	6.51	89	0	130
PC2	3	75.0	49.4	84.4	0.51	10.26	0.90	24.38	51	10.28	226	3	280
PC2	4	79.4	52.5	99.8	0.55	7.48	0.65	15.80	10	0.38	32	3	45
PC2	5	61.5	51.6	92.4	0.31	5.13	0.69	15.99	6	0.13	32	3	41
PC2	0-5	558.4	54.0	501.8	2.60	39.48	4.42	115.85	165	33.95	525	25	716
PC3	1	384.8	59.2	84.8	0.72	6.79	1.27	42.06	60	14.72	80	13	153
PC3	2	229.8	46.2	64.6	0.87	10.59	1.05	32.15	25	3.84	175	0	200
PC3	3	71.7	49.3	102.2	1.50	12.11	1.39	47.67	3	0.49	45	0	48
PC3	4	54.1	47.7	108.0	0.98	10.57	0.58	15.14	10	0.44	118	0	127
PC3	5	47.9	48.9	113.2	0.87	8.80	0.46	10.91	3	0.07	57	0	60
PC3	0-5	788.3	50.3	472.8	4.95	48.87	4.76	147.92	102	19.56	474	13	588
PC4	1	245.0	67.2	66.4	1.76	16.34	1.62	61.35	10	44.64	57	13	80
PC4	2	94.8	57.4	60.6	1.26	15.65	1.22	33.18	16	9.04	207	16	239
PC4	3	72.3	53.5	82.4	0.74	11.63	1.14	27.29	13	3.81	22	0	35
PC4	4	62.1	52.2	91.2	1.10	11.24	0.89	22.84	10	0.94	92	0	102
PC4	5	54.2	52.7	82.2	0.79	9.28	0.92	21.07	10	0.32	54	0	64
PC4	0-5	528.5	56.6	382.8	5.66	64.14	5.79	165.72	57	58.76	432	29	518
PC5	1	35.7	65.9	40.0	0.69	9.68	2.88	60.42	1396	405.04	439	29	1,863
PC5	2	32.8	45.8	74.6	0.80	11.03	2.79	55.98	283	321.39	299	3	585
PC5	3	29.6	50.6	79.4	0.65	12.61	1.39	32.02	32	24.64	83	0	114
PC5	4	37.6	47.4	94.2	1.45	13.87	0.85	21.26	6	24.83	54	0	60
PC5	5	42.4	47.3	102.0	0.39	7.80	0.83	19.24	0	0	60	0	60
PC5	0-5	178.2	51.4	390.2	3.99	55.00	8.73	188.92	1717	775.90	935	32	2,684
PC6	1	34.7	53.7	80.0	0.62	10.35	2.51	68.12	369	96.43	162	13	544
PC6	2	37.7	53.5	90.0	0.44	9.89	2.49	72.08	162	58.54	99	0	261
PC6	3	36.5	51.8	107.4	1.05	12.12	2.06	54.61	127	23.36	22	0	149
PC6	4	37.5	46.6	105.6	0.44	7.90	2.75	59.13	13	1.89	99	0	111
PC6	5	42.9	48.1	120.0	0.25	4.71	1.48	34.77	6	1.55	89	0	95
PC6	0-5	189.4	50.7	503.0	2.80	44.98	11.28	288.70	677	181.77	471	13	1,161
PC7	1	35.5	56.4	90.8	1.07	13.59	2.60	118.15	477	118.42	334	6	817
PC7	2	38.6	56.9	109.2	0.86	11.80	2.45	77.79	200	52.62	130	10	340
PC7	3	36.6	52.1	101.8	0.64	10.54	1.94	54.12	102	24.87	67	13	181
PC7	4	37.2	47.3	101.8	0.56	8.34	2.16	56.52	162	36.70	118	0	280
PC7	5	40.3	48.7	94.4	0.74	4.80	1.46	32.19	13	0.93	70	3	86
PC7	0-5	188.3	52.3	498.0	3.87	49.06	10.60	338.77	954	233.54	719	32	1,704
PC8	1	30.7	52.0	112.8	1.56	15.46	2.34	58.26	744	155.08	658	25	1,428
PC8	2	37.4	53.9	85.4	0.65	9.19	1.83	53.97	350	157.71	286	6	642
PC8	3	40.6	48.5	104.6	0.11	7.03	1.55	50.29	111	45.61	102	3	216
PC8	4	38.9	48.7	78.0	0.23	5.67	1.49	39.44	70	40.87	29	0	99
PC8	5	41.9	49.7	96.4	0.46	6.99	1.45	40.87	25	53.82	124	0	149
PC8	0-5	189.5	50.6	477.2	3.01	44.34	8.66	242.83	1301	453.09	1,199	35	2,534

Table S3 Alpha-diversity of bacterial communities along the sampled iron gradient based on OTU abundances. Shown are observed richness (nOTU), estimated richness (chao1 and ace), as well as the inverse Simpson and Shannon diversity indices.

Core ID	Depth (cm)	nOTU	chao1	ace	invS	Shannon
PC1	1	202	213	210	9.25	3.25
PC1	2	975	1,768	1,986	6.80	3.45
PC1	3	814	1,529	1,650	9.27	3.54
PC1	4	2,563	4,806	5,196	38.71	5.90
PC1	5	3,145	5,750	6,248	180.33	6.70
PC2	1	1,314	2,683	2,939	5.69	3.71
PC2	2	2,285	5,274	5,781	47.79	5.51
PC2	3	2,215	4,908	5,456	30.97	5.21
PC2	4	2,378	5,521	6,271	22.51	5.24
PC2	5	2,017	4,370	4,969	13.41	4.60
PC3	1	1,603	3,314	3,622	16.88	4.64
PC3	2	1,928	4,253	4,739	23.70	5.07
PC3	3	2,502	5,503	6,050	45.23	5.75
PC3	4	2,694	5,422	6,123	37.30	5.90
PC3	5	2,376	4,879	5,435	27.96	5.37
PC4	1	2,184	4,786	5,392	41.74	5.48
PC4	2	2,375	5,266	5,858	84.01	5.84
PC4	3	2,471	5,383	6,008	83.73	5.95
PC4	4	2,467	5,558	6,379	38.10	5.56
PC4	5	2,068	4,479	5,131	19.51	4.88
PC5	1	3,810	7,189	7,824	434.94	7.26
PC5	2	3,239	6,382	6,945	183.50	6.75
PC5	3	3,105	5,930	6,440	108.78	6.64
PC5	4	2,758	5,617	6,042	31.20	5.96
PC5	5	2,507	4,990	5,357	21.06	5.62
PC6	1	3,926	7,395	8,145	407.31	7.28
PC6	2	3,905	7,248	8,040	382.39	7.25
PC6	3	3,933	7,296	8,148	414.33	7.28
PC6	4	3,641	6,581	7,124	375.23	7.17
PC6	5	3,684	6,873	7,417	401.49	7.21
PC7	1	4,043	7,516	8,163	530.09	7.39
PC7	2	3,958	7,356	8,134	460.73	7.31
PC7	3	3,936	7,553	8,227	446.34	7.31
PC7	4	3,552	6,393	7,026	369.73	7.15
PC7	5	3,373	6,053	6,517	336.92	7.07
PC8	1	4,060	7,292	8,048	577.52	7.43
PC8	2	3,982	7,762	8,561	419.37	7.30
PC8	3	3,539	6,553	7,145	340.90	7.12
PC8	4	3,807	7,209	8,062	432.58	7.25
PC8	5	3,513	6,294	6,925	358.13	7.13

Table S4 Results of the diversity indices S (number of species), J' (evenness), $EG_{(51)}$ (expected number of genera per 52 individuals) and $H'_{(log2)}$ (heterogeneity) for the nematode community (abundance of genera) in the sediment layers (0-5 cm) of the iron-influenced (PC1-4) and unaffected sediments (PC5-8); n.n. = no nematodes.

Core ID	Depth (cm)	S	J'	$EG_{(51)}$	$H'_{(log2)}$
PC1	1	2	0.92	2.00	0.92
PC1	2	5	0.97	5.00	2.25
PC1	3	3	1.00	3.00	1.58
PC1	4	3	1.00	3.00	1.58
PC1	5	3	1.00	3.00	1.58
PC2	1	10	0.94	10.00	3.13
PC2	2	6	0.91	6.00	2.35
PC2	3	8	0.89	8.00	2.68
PC2	4	3	1.00	3.00	1.58
PC2	5	2	1.00	2.00	1.00
PC3	1	11	0.94	11.00	3.24
PC3	2	5	0.93	5.00	2.16
PC3	3	1	1.00	1.00	0.00
PC3	4	3	1.00	3.00	1.58
PC3	5	1	1.00	1.00	0.00
PC4	1	3	1.00	3.00	1.58
PC4	2	5	1.00	5.00	2.32
PC4	3	3	0.95	3.00	1.50
PC4	4	3	1.00	3.00	1.58
PC4	5	2	1.00	2.00	1.00
PC5	1	35	0.83	18.93	4.24
PC5	2	15	0.70	11.28	2.73
PC5	3	5	0.93	5.00	2.17
PC5	4	2	1.00	2.00	1.00
PC5	5	n.n.	n.n.	n.n.	n.n.
PC6	1	26	0.78	15.53	3.66
PC6	2	17	0.91	15.07	3.73
PC6	3	18	0.94	16.44	3.93
PC6	4	2	0.81	2.00	0.81
PC6	5	2	1.00	2.00	1.00
PC7	1	33	0.82	19.10	4.13
PC7	2	22	0.87	17.12	3.89
PC7	3	16	0.94	15.14	3.78
PC7	4	13	0.81	11.27	3.00
PC7	5	4	1.00	4.00	2.00
PC8	1	29	0.69	14.33	3.35
PC8	2	23	0.81	15.24	3.66
PC8	3	15	0.86	13.83	3.37
PC8	4	14	0.98	13.93	3.73
PC8	5	7	0.98	7.00	2.75

Data availability

All bacterial data is archived in the European Nucleotide Archive (ENA) under project accession number PRJEB57769, whereas all meiofaunal and environmental data is archived in the Mendeley Data Repository under the Digital Object Identifier (DOI) 10.17632/4hxhvftxbx.1

2 Figures

Figure S1 Visual representation of bacterial alpha-diversity measures along the sampled gradient. Iron-impacted and unaffected sediments are differentiated by color code, as are sediment depth horizons.

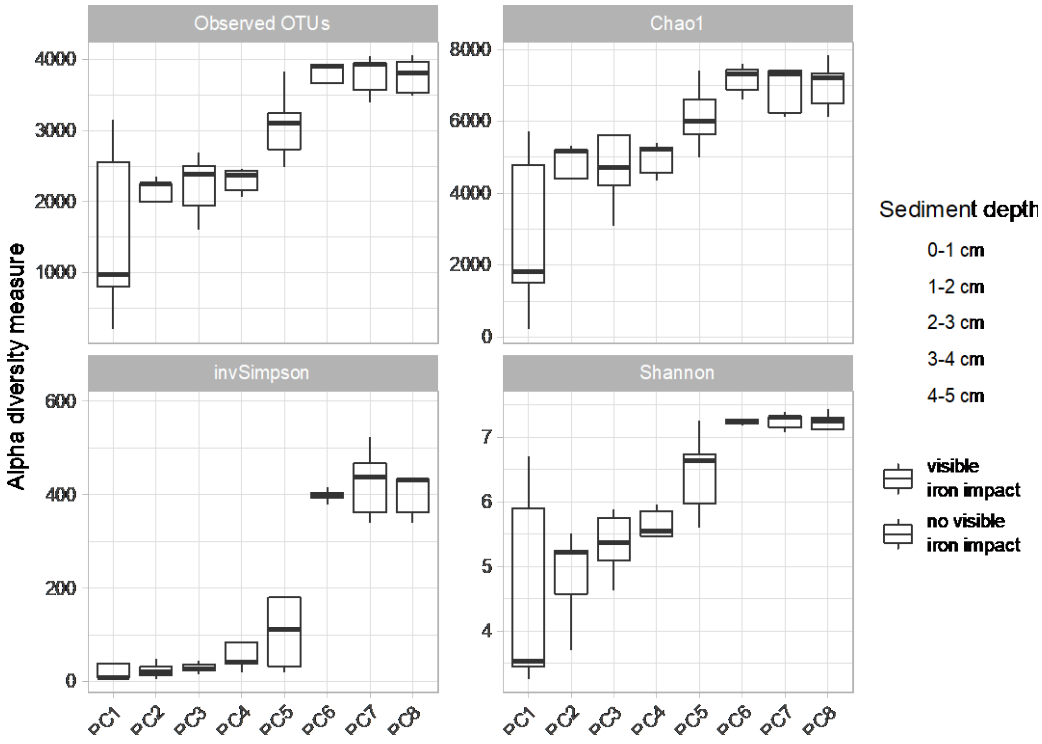

Figure S2 Dominant bacteria (>0.5% mean relative abundance in iron-enriched or unaffected sediments) that showed statistically significant differences in relative abundance between PC1-4 and PC5-8. Genera in (A) were dominant in iron-enriched sediments, and minor contributors to communities in unaffected sediments; genera in (A) were dominant members of the unaffected sediments and their relative abundance was greatly reduced under iron impact.